Methods and procedures for processing and analysing process signals in precision machining processes

Souzan Amirabadi
born on 22. September 1997
in Shiraz / Iran

Department of Electrical Engineering and Information Technology
Technische Universität Ilmenau

Advisors:

Univ.-Prof. Dr.-Ing. Giovanni Del Galdo

Dr.-Ing. Florian Römer

Dr. Marius Winter

Submission Date: 31 May 2023

Declaration

I declare that the work is entirely my own and was produced with no assistance from third parties. I certify that the work has not been submitted in the same or any similar form for assessment to any other examining body and all references, direct and indirect, are indicated as such and have been cited accordingly.

Souzan Amirabadi
Ilmenau, 31 May 2023

Acknowledgment

I would like to express my gratitude to Prof. Giovanni Del Galdo and Dr. Florian Römer for the opportunity to work on this thesis. I am also thankful to Technische Universität Ilmenau for allowing me to pursue my master’s degree. I would also like to extend my thanks to Dr. Marius Winter, and Dr. Sebastian Becker for their supervisions and assistance.

Dedication

I dedicate this thesis to my beloved mother, who has been a constant source of love, support, and encouragement throughout my academic journey. Despite the distance that separates us, her unwavering presence and belief in my abilities have been a guiding light during the challenging times. Her sacrifices and endless love have been the foundation of my determination and success. This work is a tribute to her unwavering support and serves as a symbol of my deepest gratitude.

Contents:

Abstract:

Precision machining is a manufacturing process used to produce high-precision and tight-tolerance components. Process monitoring is essential for guaranteeing the effectiveness and quality of precision machining operations.

Grinding burn, which refers to the excessive heat created during the grinding process and can cause surface damage and decreased product quality, is one of the most frequent flaws that can appear during such procedures. Grinding burn needs to be monitored during the process using the right techniques in order to avoid and reduce it.

The use of sensors to gather different types of data, including vibration, current, and acoustic emission (AE) signals, that can help analyse the grinding process is a typical method of process monitoring. Such signals are captured using specialized sensors and used as data in this thesis for additional analysis. Preprocessing is then required to improve the analysis of the collected sensor data. It involves cleansing and arranging the data in order to remove noise, identify significant segments, and extract meaningful features. This preprocessing procedure allows for a more concentrated and accurate investigation of the Grinding process, allowing for additional analysis and precised interpretation.

This thesis focuses on the preprocessing of a self-generated signal with known temporal and frequency characteristics. It provides a comparison between the performance of several time-frequency transformation methods applied to this self-generated signal, such as the short-time Fourier transform (STFT), continuous wavelet transforms (CWT), Wigner-Ville distribution (WVD), and synchrosqueezing transform (SST). It also provides an accurate evaluation of the signal's time-frequency representation (TFR). It also looks at how various time-frequency transformation algorithms can be used for process monitoring, such as detecting grinding burn.

This study investigated at different time-frequency transformation methods for determining grinding burn features. The STFT regularly demonstrated dependable TFR construction with low MSE and reduced Renyi entropy, capturing signal properties with less unpredictability. In comparison, the continuous wavelet transform (CWT) was more sporadic. With its good overall performance and faster processing, the STFT method has emerged as a viable choice for real-time monitoring applications. These findings contribute to character recognition in grinding burn, highlighting the STFT approach's potential. More study is needed to investigate alternate methods for high-frequency signal processing while taking accuracy, unpredictability, and computing time into account.

Kurzfassung:

Präzisionsbearbeitung ist ein Fertigungsprozess, der zur Herstellung hochpräziser und eng tolerierter Bauteile eingesetzt wird. Die Überwachung des Prozesses ist entscheidend, um die Effektivität und Qualität der Präzisionsbearbeitungsoperationen zu gewährleisten.

Schleifbrand, der auf übermäßige Wärmeerzeugung während des Schleifprozesses verweist und Oberflächenschäden sowie eine Verringerung der Produktqualität verursachen kann, ist eine der häufigsten Fehlerquellen, die bei solchen Verfahren auftreten können. Schleifbrand muss während des Prozesses mit geeigneten Techniken überwacht werden, um ihn zu vermeiden und zu reduzieren.

Die Verwendung von Sensoren zur Erfassung verschiedener Datenarten, einschließlich Vibration, Strom und akustischer Emissionssignale, die zur Analyse des Schleifprozesses beitragen können, ist eine typische Methode der Prozessüberwachung. Solche Signale werden mit spezialisierten Sensoren erfasst und in dieser Arbeit als Daten für zusätzliche Analysen verwendet. Anschließend ist eine Vorverarbeitung erforderlich, um die Analyse der gesammelten Sensordaten zu verbessern. Dabei werden die Daten gereinigt und geordnet, um Rauschen zu entfernen, signifikante Segmente zu identifizieren und sinnvolle Merkmale zu extrahieren. Durch dieses Vorverarbeitungsverfahren wird eine konzentriertere und genauere Untersuchung des Schleifprozesses ermöglicht, die zusätzlichen Analysen und präzise Interpretationen zulässt.

Diese Arbeit konzentriert sich auf die Vorverarbeitung eines selbst generierten Signals mit bekannten zeitlichen und frequenzspektralen Eigenschaften. Es erfolgt ein Vergleich der Leistung mehrerer Zeit-Frequenz-Transformationsmethoden, die auf dieses selbst generierte Signal angewendet werden, wie beispielsweise die Kurzzeit-Fourier-Transformation (STFT), kontinuierliche Wavelet-Transformationen (CWT), Wigner-Ville-Verteilung (WVD) und Synchrosqueezing-Transformation (SST). Es erfolgt auch eine genaue Bewertung der Zeit-Frequenz-Darstellung (TFR) des Signals. Es wird auch untersucht, wie verschiedene Zeit-Frequenz-Transformationsalgorithmen zur Prozessüberwachung verwendet werden können, beispielsweise zur Erkennung von Schleifbrand.

Diese Studie untersuchte verschiedene Zeit-Frequenz-Transformationsmethoden zur Bestimmung von Merkmalen des Schleifbrands. Die STFT zeigte regelmäßig eine zuverlässige TFR-Konstruktion mit geringem MSE und reduzierter Renyi-Entropie, wodurch Eigenschaften des Signals mit geringerer Unvorhersagbarkeit erfasst wurden. Im Vergleich dazu war die kontinuierliche Wavelet-Transformation (CWT) unregelmäßiger. Mit ihrer guten Gesamtleistung und schnelleren Verarbeitung hat sich die STFT-Methode als eine geeignete Wahl für Echtzeitüberwachungsanwendungen herausgestellt. Diese Erkenntnisse tragen zur Zeichenerkennung bei Schleifbrand bei und unterstreichen das Potenzial des STFT-Ansatzes. Weitere Untersuchungen sind erforderlich, um alternative Methoden für die Hochfrequenz-Signalverarbeitung unter Berücksichtigung von Genauigkeit, Unvorhersagbarkeit und Rechenzeit zu erforschen.

1. Introduction:

1.1 Motivation and Objective

Precision machining processes have become an integral part of modern manufacturing.[1] These processes enable the production of high-quality, high-precision, and tight-tolerance components required for a variety of aerospace, medical device, and automotive applications. [2] However, various parameters such as cutting speed, feed rate and tool wear must be tightly controlled and monitored to achieve the required accuracy. Variations in these parameters can lead to poor product quality, lost production, and increased costs. [3]

In the last decade, considerable progresses in sensor and signal processing technology have enabled real-time data collection and analysis during precision processing. This data can be used to monitor the process in real time, detect process anomalies, and optimize processing parameters. [4] Signal processing, as a part of process monitoring, plays a crucial role in improving the efficiency and accuracy of precision machining processes. [5] By processing and analysing process signals, the number of defective products would be reduced, production losses would be minimized and as a result, the overall performance of the processing system would be improved. [6]

The processing and analysis of process signals in precision machining processes is an important topic of research. This research enables the identification of process changes and the detection of process anomalies. Signal processing and analysis have been used in different aspects of precision machining, including process monitoring, tool condition monitoring [7], and surface roughness prediction. [8] Various signal processing techniques have been developed for precision machining, such as time-domain analysis, frequency-domain analysis, and time-frequency analysis. Several signals, including vibration, current, AE, and temperature, can be evaluated to obtain insight into the grinding process. [9] However, the primary focus of this thesis will be on the analysis of vibration, current, and AE signals. The reasoning behind this decision will be addressed in depth in Chapter 2.1.

The complexity and high sampling rate of process signals caused difficulties in determining the best time-frequency transformation for a fair comparison, which was a main topic addressed in this research. To overcome this challenge and permit a more exact evaluation, a self-generated signal with established temporal and frequency characteristics was used. Working with a self-generated signal ensured extensive information and control over all aspects of the signal, allowing for more exact interpretation and evaluation of various time-frequency transformation approaches.

The primary objective of this thesis is to conduct a comprehensive investigation into the latest time-frequency transformation methods such as STFT, CWT, WVD, EMD and SST and procedures utilized for the processing and analysis of process signals in precision machining processes. This study endeavours to analyse the benefits and limitations of each approach. The research approach is to comprise a thorough review of the current literature on several time-frequency transformations on signal and analysis techniques. Additionally, the research provides a detailed description of a comparison of the quality and complexity of various pre-processing methods obtained from relevant case studies and experiments about

1.2 Thesis outline

The subsequent chapters of this study are structured as follows: Chapter 2 gives a thorough review of the state-of-the-art in precision machining, including the machining procedures, and the factors that affect machining performance and result in burn. This chapter will also go into the principles of signal sources in machining processes and signal acquisition, giving insights into the different types of signals produced during machining operations and the techniques used to capture and record them. A thorough study of other time-frequency transformation methods, such as FFT, CWT, WVD, SST, and others, will also be covered. These methods are essential for assessing the dynamic properties and behaviour of signals in the time and frequency domains. Chapter 3 presents an in-depth review of the state of the research on time-frequency transformation methods and analysis that are used in precision machining processes. Chapter 4 outlines the evaluation of preprocessing approaches used for comparing of methods. Furthermore, this chapter presents a series of case studies and experiments that demonstrate the effectiveness of these methods. Chapter 5 discusses the research results and provides recommendations for the selection of appropriate signal processing and analysis techniques in precision machining. Lastly, Chapter 6 presents a comprehensive conclusion based on the results obtained from the evaluation of the different methods.

In summary, this chapter presents an outline of the thesis, including motivation and research aims. It outlines the thesis's structure and organization.

2. State of the art

Precision machining processes are critical to producing high precision, high quality components. Manufacturing products with complex shapes and dimensional tolerances requires high-precision machining processes. Various processes are used such as turning, milling, grinding and EDM machining. [10] A key factor in achieving precision is the use of high-precision machine tools and cutting tools that are constantly being developed and improved. Additionally, metrology and quality control play a key role in ensuring the accuracy of the final product. In the field of precision machining, research is underway to improve the efficiency and accuracy of these processes, especially for micro- and nanoscale applications. [11]

Precision machining research efforts are focused on improving the efficiency and accuracy of these processes, particularly in micro- and nanoscale applications. [11] Methods for transforming time to frequency have emerged as useful tools in this endeavour. These methods offer a complete evaluation of the dynamic behaviour of the process by examining the time-varying frequency content of machining signals. Time-frequency transformations display the frequency characteristics and temporal changes of machining signals, helping in process optimization and fault detection.

The following steps outline the process involved in the analysis and characterization of the grinding process. Detailed explanations and in-depth discussions regarding each step will be provided in the following chapters.

1. The grinding process is the primary method of machining.
2. Sensor data collection: During the grinding process, various sensors (vibration, current, and sound emission, temperature, etc.) are employed to acquire raw signals.
3. Preprocessing: The acquired raw signals are subjected to preprocessing processes such as filtering and denoising to remove noise and improve signal quality.
4. Time-frequency transformation: To examine the frequency content over time, the preprocessed signal is transformed into several time-frequency representations.
5. Time-frequency representation evaluation: To analyse the quality and properties of the produced time-frequency representations, numerical metrics such as Renyi entropy, mean squared error, and calculation time are used.
6. Feature extraction: a kind of preprocessing; the process of extracting features from time-frequency representations for use in machine learning or other analysis approaches, which is out of scope of this thesis.

2.1 Grinding Process and challenges

Grinding is a sophisticated machining process that is utilized in many industries to produce precise finishes and accurate dimensions on workpieces. The process involves the use of a rotating grinding wheel that removes material from the surface of the workpiece through the action of abrasive particles. This precise and efficient method is widely used to achieve the desired surface qualities. [12]

Despite the many benefits of grinding, several defect types can arise during the grinding process, including chatter, tool wear, wheel glazing, wheel loading, and surface/subsurface cracks. Chatter is the vibrating or unstable behaviour of the grinding wheel that results in irregular material removal and poor surface quality. Tool wear refers to the slow degradation of the abrasive wheel, which results in a loss of dimensional accuracy and surface quality. When material accumulates on the grinding wheel, it reduces its cutting ability. When the grinding wheel becomes clogged with workpiece material or swarf, its cutting performance decreases. Excessive grinding pressures, high temperatures, or insufficient cooling can cause surface and subsurface fissures, jeopardizing the mechanical characteristics and integrity of the completed product. [13]

Grinding burn is one of these defect variations that demands specific care. Burn in grinding refers to the undesirable thermal damage caused by high temperatures during the grinding process, which can negatively impact the quality and performance of the finished product. Burn can cause microstructural changes in the workpiece, leading to reduced mechanical properties and decreased surface integrity. As such, it is important to minimize the risk of burn in grinding operations to ensure the quality and reliability of the final product. [14]

To detect and prevent burning, signal processing has emerged as a promising solution. By analysing current, vibration, and structure-borne noise signals, signal processing can provide valuable insights into the state of the grinding process, allowing for early detection and prevention of burning. The use of signal processing technology allows for real-time monitoring of the grinding process, enabling operators to make quick and informed decisions to minimize the risk of burning and improve the efficiency of the manufacturing process. [15]

The signals recorded during grinding exhibit non-stationary and non-transient behaviour due to the constantly changing grinding conditions, including wheel wear, vibration, and thermal effects. A non-stationary signal is one whose statistical properties change over time, making it unpredictable and difficult to model. This can occur in signals such as vibration, where changes in mean, variance, or autocorrelation can be caused by factors such as wheel wear or changes in the depth of cut. [16]

Similarly, a non-transient signal is one that exhibits behaviour that changes over time and depends on initial conditions. For example, the AE signal during the initial stage of grinding may exhibit transient behaviour as the grinding wheel makes contact with the workpiece. Once the system reaches a steady-state behaviour, it becomes non-transient, and the signal becomes more predictable. This behaviour causes the signals to have time-varying frequency content, which makes it challenging to analyse using traditional frequency domain methods like Fourier Transform. [17]

2.2 Data Collection

Acquiring data from sensors is an important step in research. Sensors are devices that measure various physical quantities such as temperature, pressure, force, and vibration. These sensors are used to collect data during the grinding process, and the collected data is analysed to obtain relevant features for further processing. [18]

Temperature measurement during the machining process might be technically challenging. Temperature variations during grinding can be influenced by parameters such as cutting speed, feed rate, and material properties, making accurate measurement and interpretation of temperature data difficult. Furthermore, incorporating temperature sensors into the grinding setup may bring complications and potential interferences. [19]As a result, in the context of this study, the emphasis is on the sensors, such as vibration, current, and AE, which provide immediate and trustworthy information about grinding burn detection. [14]

The specific sensors used in this study are current sensors, vibration sensors and AE sensors.

- Current sensors, such as a current transformer (CT) or a Hall Effect sensor, can be used to measure the current flowing through the grinding machine's electric motor. This information can be used to determine the machine's energy consumption and detect any motor problems such as overloads that can affect the grinding process and material quality.
- The vibration generated by the grinding machine can be measured using vibration sensors such as accelerometers. This information can be used to calculate the level of vibration generated during the grinding process and identify machine issues such as misalignment and worn bearings that can affect the grinding process and material quality.

- AE sensors, such as contact microphones, can be used to measure the sound and vibration generated by the grinding process and transmitted through the structure of the machine and the material. This information can be used to determine the level of sound and vibration generated during the grinding process, and to identify any issues with the machine or the material, such as chatter or cracking, which can affect the quality of the material.

It is also important to note that all sensors should be properly calibrated and connected to the right data acquisition equipment to ensure the data collected is accurate and reliable.

In this study, the data collection involved acquiring a real-world signal that had not undergone any significant pre-processing. The signal was then segmented to extract a portion of interest, which was used for further analysis. The segmentation process involved selecting a 0,5-second region in the middle part of the signal. As the steady stage of the grinding operation, the middle part of the signal is chosen for analysis while the initial and final portions exhibit transient features as a result of workpiece positioning or grinding wheel acceleration. Any anomalies or artifacts in the signals that could be present during those periods can be efficiently removed by eliminating these transitional phases. [20]

2.3 Signal transformation methods

The analysis and processing of signals is a critical aspect of many fields, including engineering, physics, and biology. With the increasing complexity of modern data, it has become increasingly important to develop techniques for time-frequency analysis that are both accurate and efficient. In response, researchers have proposed a range of methods, each with its own strengths and weaknesses. Time-frequency analysis is a fundamental tool in the study of signals and systems and has numerous applications in fields ranging from telecommunications to biomedical engineering. [21] In this chapter, some of the most prominent time-frequency transformation methods that have been developed to date, are reviewed, which are aimed at extracting valuable information from signals.

The table provided below summarizes various signal processing techniques used in this research to analyse and transform signals. These techniques are categorized into linear and non-linear distributions, reassignment methods, and multi-resolution analysis.

Table 1 Overview of different type of methods/Distributions

#	Type	Distribution/ Transform
1	Linear Distributions	Fourier Transform
		Gabor Transform
		Wavelet Transform
		Wavelet Packet Transform
		Chirplet Transform
		Cosine Packet Transform
2	Non-linear Distributions	Wigner-Ville Distribution
		Margenau-Hill Distribution

		Choi-Williams Distrbution
3	Reassignment Methods	Synchro-squeezed Transform
		Synchro-extracted Transform
4	Multi-Resolution Analysis	Empirical Mode Distribution
		Variational Mode Distribution

2.3.1 Linear Distributions

2.3.1.1 Fourier transform

The Fast Fourier Transform (FFT) is a widely used tool for analyzing stationary signals. [22] It works by decomposing a signal into its frequency components, providing useful information about its spectral content. However, it assumes that the signal is stationary, meaning that its statistical properties do not change over time. [23] In reality, many signals in practical applications are non-stationary, including machining process signals. [5] Non-stationary signals pose a challenge for the FFT because it assumes that the signal is time-invariant. [23] To obtain a more accurate representation of their spectral content, alternative techniques suitable for the analysis of non-stationary signals should be considered. As such, the following chapters will provide an explanation of these methods and their application in analysing non-stationary signals. [24]

2.3.1.2 Gabor transform

The STFT is a frequently used time-frequency analysis approach in signal processing that provides useful insights into the spectral content of a signal across time. It enables us to investigate how the frequency components of a signal change over time. The STFT accomplishes this by applying a window function to small portions of the signal and then computing the Fourier transform of each windowed segment.[25]

The STFT of a continuous-time signal x(t) can be described mathematically as follows in (1):

$$STFT(t,\omega) = \int_{-\infty}^{\infty} x(\tau) w(\tau - t) e^{-j\omega\tau} d\tau \tag{1}$$

where t is the time variable, represents the angular frequency variable, $x(t)$ denotes the input signal, and $w(t)$ is the window function. [26]

When using the STFT analysis, researchers have numerous window functions to choose from. In terms of the resulting TFR each window function has advantages and downsides. The rectangular window, Hamming window, Hanning window, and Blackman window are all typical window functions. The proper window is chosen based on the analysis's specific requirements and the trade-off between frequency resolution and spectral leakage suppression. Researchers frequently experiment

with several window functions to find the one that best suits their specific application and signal characteristics.
The choice of window size and overlapping size in the STFT analysis is critical in determining the time and frequency resolution of the TFR. [27]

The window size, relates to the length of the window function w(t) applied to the signal during the STFT analysis. The size of the window has a major impact on the resolution in both the time and frequency domains.
In terms of time resolution, a bigger window size allows for improved frequency resolution, allowing for the detection of finer frequency details in the resulting TFR. This is due to the longer window collecting more oscillations within the windowed section, resulting in a more accurate calculation of frequency components. A larger window size, on the other hand, comes at the cost of poorer time resolution because it encompasses a larger amount of the signal. Rapid changes in the signal inside the window may not be caught as precisely. [28]

With a larger window size, the STFT offers superior frequency discrimination. This is because a bigger window size leads to narrower frequency bins in the TFR. As a result, closely spaced frequency components can be separated better, allowing for more precise identification of individual frequency components.

In the STFT analysis, the overlapping size specifies the degree of overlap between neighbouring windows. It is critical in the trade-off between time and frequency resolutions.
Increasing the overlapping size results in a higher time resolution in the final TFR. This is because more overlap between windows allows for more frequent signal sampling, allowing for the capture of quick temporal changes with greater precision. However, increasing the overlapping size brings redundant information from surrounding windows, potentially leading to greater computing complexity.

The overlapping size, on the other hand, has an effect on the frequency resolution of the STFT. The frequency resolution reduces as the overlap between windows grows. This is because surrounding frequency components become less apparent, resulting in a decrease in frequency discrimination. [28]

To select appropriate values for the window size and overlapping size, examine the specific requirements of the investigation as well as the characteristics of the signal being studied. When high resolution is required, such as when analysing transitory signals, smaller window sizes are desirable. Larger window sizes, on the other hand, are more suited to catching fine frequency information in signals with stable spectral components. The overlapping size is chosen based on the desired trade-off between time and frequency resolutions that matches the research objectives and the characteristics of the signal under examination.

Understanding the effects of window size and overlapping size on time and frequency resolutions enables researchers and practitioners to make informed decisions when applying the STFT to different signals, tailoring the analysis parameters to best suit the specific characteristics and objectives of the study. [25]

2.3.1.3 Wavelet transform

Unlike STFT, which has resolution limitations, wavelet transforms use variable window sizes with wavelet functions. WT can be described as the correlation between a signal and a set of fundamental wavelets. A wavelet is a localized wave, i.e., a signal with zero mean that decays to zero after a few oscillations. The wavelet transform is defined in a similar way to the Fourier transform, but instead of using harmonics, a mother wavelet is used. The mother wavelet function is denoted by Ψ. [29]

$$CWT(a,b) = \frac{1}{\sqrt{a}} \int_{-\infty}^{\infty} x(t) \Psi_{a,b}(\mathrm{t}) dt \tag{2}$$

$$\Psi_{a,b}(t) = \frac{1}{\sqrt{|\ a\ |}} \Psi\left(\frac{t-b}{a}\right) \tag{3}$$

where $x(t)$ is the signal being analysed, $\Psi(t)$ is the analyzing wavelet, a is the scale parameter, and b is the translation parameter. The b parameter affects the position of the wavelet function as it is transformed across the signal and provides time information in the wavelet transform. The scale parameter s expands (widens) or compresses the signal. [30] A large scale provides low frequency information, and a small scale provides high frequency information. The CWT was developed for analysing transient signals with variable window sizes and has the ability to identify frequency components simultaneously with their time locations. [31] CWT uses the wavelet function Ψ(t) to generate a scalogram similar to the spectrogram in time-frequency analysis.

Wavelets have distinct properties that make them useful for a wide range of signals and applications. The formula and shape of some of the wavelets are shown in Table 2 below.

Table 2 overview of some frequently used Wavelets

Wavelet	Formula	Shape
Daubechies	$\psi(t) = \sum_{k=0}^{N-1} h_k \cdot \phi(2t-k)$	Smooth, compact support, orthogonality
Haar	$\psi(x) = \begin{cases} 1 & 0 \leq x < \frac{1}{2} \\ -1 & \frac{1}{2} \leq x < 1 \\ 0 & otherwise \end{cases}$	Piecewise constant, abrupt transitions
Morlet	$\psi(t) = A \cdot \exp\left(-\frac{t^2}{2\sigma^2}\right) \cdot \cos(2\pi f_0 t)$	Oscillatory, Gaussian envelope
Complex Morlet	$\psi_\sigma(t) = c_\sigma \pi^{\frac{-1}{4}} e^{\frac{-1}{2}t^2}\left(e^{i\sigma t} - \kappa_\sigma\right)$	oscillatory

The Daubechies wavelet is a popular wavelet. The compact support and orthogonality qualities of Daubechies wavelets make them ideal for representing and evaluating signals with sharp transitions or discontinuities. They are frequently used for image compression, denoising, and feature extraction. [32]

Another frequent choice in time-frequency analysis is the Morlet wavelet. Morlet wavelets are created by modulating a complicated sinusoidal carrier with a Gaussian envelope. They are well-suited for collecting oscillatory components in signals, such as in EEG or neural activity analysis. The complex Morlet wavelet contains magnitude as well as phase information, allowing for extensive time-frequency analysis. [33]

The Haar wavelet is a straightforward and efficient wavelet that is well-suited for assessing signals with sudden changes or step-like properties. Its piecewise constant shape is distinguished by positive and negative sections separated by an abrupt transition. The Haar wavelet is a computationally efficient wavelet that is commonly used in image and signal compression, edge detection, and feature extraction. [34]

There is a real Morlet wavelet in addition to the complex Morlet wavelet and the Haar wavelet. Taking the real component of the complicated Morlet wavelet yields real Morlet wavelets. They provide a real-valued representation while keeping the complex Morlet wavelet's time-frequency features. This makes them appropriate for time-frequency analysis jobs that require a real-valued output or for examining oscillatory components in the frequency domain. [35]

The wavelet used is determined by the individual properties of the signal as well as the analytic goals. The Daubechies wavelet is appropriate for signals with sharp transitions or discontinuities, the Morlet wavelet is effective for capturing oscillatory components, the Haar wavelet is appropriate for signals with abrupt changes or step-like features, and the real Morlet wavelet represents oscillatory components in real time.

Understanding the features of various wavelets assists scientists and engineers in selecting the best wavelet for their signal processing and time-frequency analysis jobs. Each wavelet type has distinct characteristics and can provide useful insights into the frequency content and temporal evolution of the signals under consideration.

However, wavelet transform also has some disadvantages compared to STFT. One of the main disadvantages is that it may be more computationally intensive and harder to implement than the STFT. Additionally, the choice of wavelet function can affect the results of the transform and the interpretation of the results may be more complex to interpret. [36]

In this thesis, the focus is primarily on the Complex Morlet wavelet. The Complex Morlet wavelet was chosen because of its attractive properties for time-frequency analysis. The Complex Morlet wavelet provides a good balance of temporal and frequency localization, making it useful for evaluating signals with time-varying spectral content. Its wavelet formula can be seen in table (2) and its important parameters are defined as below: [35]

$$\kappa_\sigma = e^{-\frac{1}{2}\sigma^2} \tag{4}$$

$$c_\sigma = \left(1 + e^{-\sigma^2} - 2e^{-\frac{3}{4}\sigma^2}\right)^{\frac{-1}{2}} \quad (5)$$

κ_σ is defined by the admissibility criterion, and the normalisation constant c_σ is the parameter σ in the Morlet wavelet allows trade between time and frequency resolutions. Conventionally, the restriction $\sigma > 5$ is used to avoid problems with the Morlet wavelet at low σ (high temporal resolution) [37]

The Gaussian envelope allows for a localized representation of the signal's time-varying spectral components while sacrificing time and frequency resolution.

This thesis tries to capture the complicated dynamics and spectral changes found in the signals under examination by employing the Complex Morlet wavelet by changing its main parameter. The wavelet's capacity to offer simultaneous time and frequency information is useful for non-stationary signal analysis, detecting transitory occurrences, and defining oscillatory phenomena.

2.3.1.4 Chirplet

The Chirplet Transform (CT) is a signal processing method that examines signals in the time-frequency domain. It is a generalization of the wavelet transform that uses chirp signals as its basis functions. Chirp signals allow the CT to break down a given signal into a collection of chirplets with various time-varying frequencies and amplitudes. Chirp signals are defined by their fluctuating frequency over time.

The CT operates mathematically by convolving a signal with chirplets that have predefined center frequencies, time-varying frequencies, and bandwidth. TFR of the signal are created by projecting the resulting convolutions onto a time-frequency plane. [38]

Analyzing signals displaying phenomena like frequency modulation, amplitude modulation, or instantaneous frequency shifts is made particularly advantageous by the CT's capacity to capture time-varying frequency components. The CT allows for exact localisation and tracking of these time-varying features by breaking the signal down into chirplets, which enables in-depth investigation of the signal's dynamics. It is also robust to noise and can accurately analyse signals with a low signal-to-noise ratio.

Numerous industries use the CT, including communication systems, radar signal processing, biomedical signal analysis, and audio processing. The CT improves target signature extraction and provides precise target velocities for radar applications. It assists in the identification and categorization of transient events in biomedical signal analysis, such as abnormal electrocardiogram (ECG) readings or seizure activity. The CT is used in communication systems for interference detection, channel estimation, and signal modulation and demodulation. the CT coefficients. The CT coefficients represent the time-varying frequency content of the signal and can be used to analyse non-stationary signals such as those found in radar, sonar, and seismic applications. [39]

However, the CT has some limitations. One limitation is that it requires a large number of chirplets to accurately represent the frequency content of a signal, which can be computationally expensive. Additionally, the choice of chirplets and their parameters can impact the accuracy of the results obtained through CT. Furthermore, the CT is limited to analysing signals with a single chirp, which can be a disadvantage for signals with multiple chirps. [40]

2.3.1.5 Cosine Packet Transform

The Cosine Packet Transform (CPT) is a signal processing technique that allows the analysis of signals in the time-frequency domain using cosine signals as basis functions. The CPT is a generalization of the Discrete Cosine Transform (DCT), which is a popular transform used in image and video compression. The CPT decomposes a signal into a set of cosine packets with varying frequency and time support.

The CPT works by convolving a signal with a set of cosine packets that have different frequencies and time supports. The resulting convolutions are then projected onto a time-frequency plane to obtain the CPT coefficients. The CPT coefficients represent the time-frequency content of the signal and can be used to analyze signals with non-stationary frequency content. [41]

One of the main advantages of the CPT is its ability to represent signals with a small number of coefficients, which makes it computationally efficient. Additionally, the CPT is well-suited for signals that have energy concentrated in specific frequency bands. This makes it a useful tool for analyzing signals such as speech and audio.

However, the CPT has some limitations. One such limitation is its sensitivity to noise, which can result in inaccurate representations of the time-frequency content of the signal. Additionally, the CPT is not suitable for analyzing signals with rapidly changing frequency content, as it can result in poor time-frequency resolution. Furthermore, the choice of cosine packets and their parameters can impact the accuracy of the results obtained through CPT. [42]

2.3.1.6 Wavelet Packet Transform

Wavelet Packet Transform (WPT) is a signal processing technique that decomposes a signal into a set of wavelet packets. Unlike the traditional wavelet transform, which decomposes a signal into a set of wavelet coefficients, WPT decomposes a signal into a tree-like structure of wavelet packets. This structure allows for more flexibility in analyzing the frequency content of a signal, making it a powerful tool in various fields such as signal processing, image compression, and pattern recognition.

WPT works by decomposing a signal into a set of wavelet packets using a series of high-pass and low-pass filters. The high-pass filter separates the high-frequency components of the signal, while the low-pass filter separates the low-frequency components. This process is repeated iteratively, resulting in a tree-like structure of wavelet packets as shown in Figure 1. Each wavelet packet represents a sub-band of the signal, and the nodes at the bottom of the tree represent the smallest sub-bands. [43]

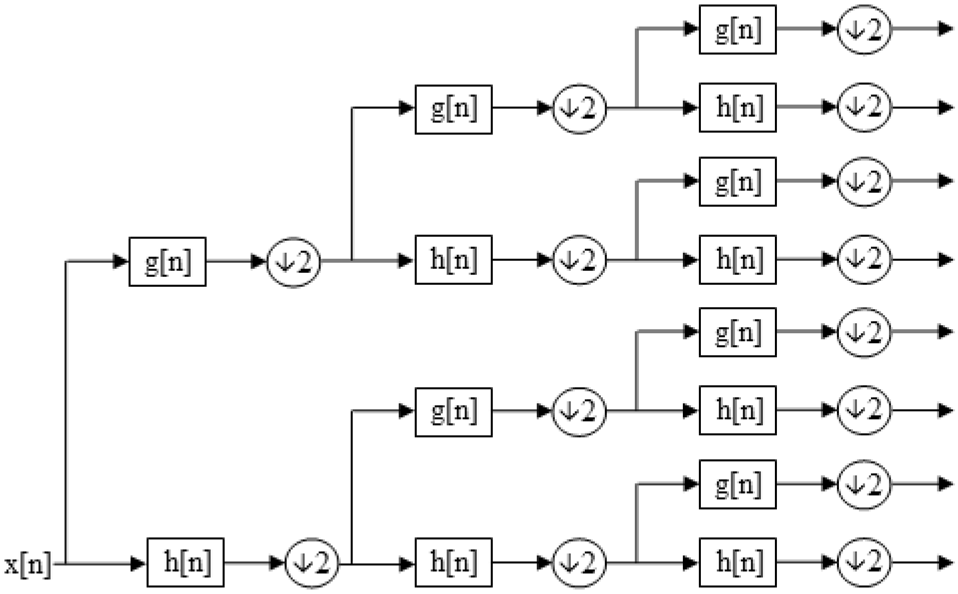

Figure 1 tree structure of WPT

One of the advantages of WPT is that it provides a more detailed analysis of the frequency content of a signal compared to the traditional wavelet transform. This is because WPT allows for the decomposition of a signal into finer frequency sub-bands. WPT also allows for the extraction of important features of a signal, making it a useful tool in pattern recognition and classification tasks. [44]

However, there are also limitations to WPT. One of the main limitations is that the tree-like structure of wavelet packets can be computationally expensive, especially for signals with a large number of samples. Additionally, the choice of wavelet basis and filter parameters can impact the accuracy of the results obtained through WPT. Furthermore, WPT suffers from the same limitations as the traditional wavelet transform, such as the inability to handle non-stationary signals and the sensitivity to noise. [43]

2.3.2 Non-Linear Distribution

The theory of non-linear time-frequency transformations is typically grounded in quantity mechanics, and operators' theory can be employed for both derivation and computation purposes. The theoretical framework proposes that any quadratic transformation that is both time and frequency invariant can be represented in (6):

$$C_x(t,f) = \int_{-\infty}^{\infty} \int_{-\infty}^{\infty} A_x(\eta,\tau)\Phi(\eta,\tau)e^{-j2\pi(\eta t+\tau f)}\, d\eta d\tau \tag{6}$$

In this context, the time frequency representation of the signal is denoted by $C_x(t,f)$. The symbol τ is used to represent time-shifting, while j represents the imaginary unit. Additionally, η represents frequency shifting, and $\Phi(\eta,\tau)$is the kernel function of a specific time-frequency transformation. Finally, $A_x(\eta,\tau)$ is used to represent the ambiguity function. This function is represented in (7):

$$A_x(\eta,\tau) = \int_{-\infty}^{\infty} x\left(t+\frac{\tau}{2}\right) x^*\left(t-\frac{\tau}{2}\right) e^{j2\pi\eta t} dt \tag{7}$$

It is important to note that this function first measures time-frequency correlation of the signal or reflects the degree of similarity between the signal and its shifted counterpart in the time-frequency plane and then applies a Fourier transform. Essentially, it denotes the Fourier transform of the autocorrelation function of time and frequency. The kernel function $\psi(\eta,\tau)$ serves both the purpose of uniquely specifying the characteristics of a given transformation and determining the appropriateness of specific transformations. [45]

2.3.2.1 Wigner-Ville Distribution, Pseudo Wigner-Ville Distribution

The Wigner-Ville distribution (WVD) is a TFR of a signal that was first introduced by Eugene Wigner in 1932 and later modified by Jean Ville in 1948. The WVD is a complex-valued function that is used to analyse the time-frequency characteristics of a signal. In this scenario, the WVD can be obtained by performing a Fourier transformation on the instantaneous autocorrelation function of the signal. [46] The WVD can be seen as a special example of the Cohen distribution with a unity kernel function as in (8) shows and its characteristics can be studied in the same way [47]

$$WVD(f,t) = \int x\left(t+\frac{\tau}{2}\right) x^*\left(t-\frac{\tau}{2}\right) e^{-j2\pi f\tau} d\tau \tag{8}$$

This requires a large amount of computational power, especially for signals with a large number of samples.

The energy and phase information of the signal is preserved by the WVD, which is commonly lost due to windowing and scaling in the STFT and WT. The WVD also provides high-resolution analysis in the temporal and frequency domains, which allows for capture of slight signal changes. [48]

While the WVD has many advantages, it is nonetheless vulnerable to cross-terms, which are interference terms that manifest themselves when the signal has more than one component.

To understand why interferences, arise, consider two sinusoidal components with comparable frequencies but different phases:

$$x_1(t) = A_1 \cos(\omega_1 t + \phi_1)$$

$$x_2(t) = A_2 \cos(\omega_2 t + \phi_2)$$

where A1 and A2 are the amplitudes, 1 and 2 are the angular frequencies, and 1 and 2 are the sinusoidal component phase offsets.

The WVD formula determines the instantaneous energy contributions at different time-frequency points when these sinusoidal components overlap in time. WVD for the sinusoids that overlap is computed as:

$$WVD(t,\omega) = \int \left[x\left(t+\frac{\tau}{2}\right) x^{*}\left(t-\frac{\tau}{2}\right) e^{-j\omega\tau} \right] d\tau \tag{9}$$

By substituting the overlapping sinusoids into the WVD formula, the resulting expression becomes:

$$\begin{aligned} WVD(t,\omega) = \int \Bigg[& \left(A_1 * cos\left(\omega_1\left(t+\frac{\tau}{2}\right)+\phi_1\right)\right) \\ & * \left(A_2 * cos\left(\omega_2\left(t-\frac{\tau}{2}\right)+\phi_2\right)\right) * e^{-j\omega\tau} \Bigg] d\tau \end{aligned} \tag{10}$$

Extending the above statement yields:

$$\begin{aligned} WVD(t,\omega) = \int \Bigg[& A_1 * A_2 * cos\left(\omega_1\left(t+\frac{\tau}{2}\right)+\phi_1\right) \\ & * cos\left(\omega_2\left(t-\frac{\tau}{2}\right)+\phi_2\right) * e^{-j\omega\tau} \Bigg] d\tau \end{aligned} \tag{11}$$

the expression can be further reduced by using the trigonometric equation $cos(A) * cos(B) = (1/2) * (cos(A + B) + cos(A - B)$:

$$\begin{aligned} WVD(t,\omega) = & \frac{1}{2} * A_1 * A_2 \\ & * \int \big[cos\big((\omega_1-\omega_2)t + (\phi_1+\phi_2)\big) * e^{-j\omega\tau} \\ & + cos\big((\omega_1+\omega_2)t + (\phi_1-\phi_2)\big) * e^{-j\omega\tau} \big] d\tau \end{aligned} \tag{12}$$

In the overlapping regions, the interference term $cos\big((\omega_1+\omega_2)t + (\phi_1-\phi_2)\big) * e^{-j\omega\tau}$ appears. The modulation or beat-like pattern that occurs when the sinusoidal components overlap is represented by this interference term.

The interference is caused by the multiplication of the two sinusoids, which results in the formation of new frequency components. These intermodulation products help to explain the interference patterns found in the WVD's overlapping regions.

Understanding the interference effects allows researchers to interpret and analyse the TFR more correctly. Researchers can determine the inherent properties of the signal and separate them from the interference effects by analysing the interference patterns created by overlapping sinusoidal components.

In addition, the WVD's high computational complexity as said before, necessitates more time and effort to implement than alternative transformation strategies.

Cross-term interference is a problem for the WVD, which means that having numerous signal components can lead to erroneous peaks or ridges in the time-frequency plane that don't represent any physical reality. By applying windows to the signal in the time and frequency domains as represented in (13), the Pseudo Wigner-Ville Distribution (PWVD) seeks to minimize or completely remove the cross-term interference. [49]

$$PWVD(t,f) = \int x(\tau)x^*(\tau - t)h(t,\tau)e^{-i2\pi f\tau}\, d\tau \tag{13}$$

A window function called *h(t)* is used to window the signal in the temporal domain and reduce cross-term interference.

There are several techniques to optimize the windows for various purposes, and the choice of the windows influences the resolution and accuracy of the PWVD. The instantaneous frequency, bandwidth, and modulation of the signal, as well as other time-frequency features like its modulation, can all be more clearly and accurately depicted by the PWVD than by the WVD. [50]

2.3.2.2 Margenau-Hill transformation

The Margenau-Hill distribution is a member of Cohen's class distributions, which encompasses time-frequency transformation that utilize a kernel function as shown in (12) to process signals. [51]

$$\Phi(\eta,\tau) = cos\left(\frac{\eta.\tau}{2}\right) \tag{14}$$

The Margenau-Hill distribution plays a significant role in effectively reducing interferences that may arise in TFR.[45]

2.3.2.3 Choi- Williams Distribution

One of the members of Cohen's class distribution function is the Choi-Williams distribution function. [52] Hyung-Ill Choi and William J. Williams first put forth the idea in 1989. As can be seen in (15) This distribution function uses an exponential kernel to suppress the cross-term.

$$\Phi(\eta,\tau) = e^{-\alpha(\eta.\tau)^2} \tag{15}$$

It should be noticed that in the ambiguity domain, the kernel gain, which denotes the degree of suppression, does not decrease uniformly along the axes. As a result, the Choi-Williams distribution function's kernel function is most useful for eliminating cross-terms caused by signal components with different time and frequency centres. [53] The Choi-Williams distribution function, in other words, is effective at reducing interference between signal components that display different oscillations in both time and frequency. [54]

2.3.3 Reassignment Methods

2.3.3.1 SST + Formula

The Synchrosqueezed Transform (SST) is a time-frequency analysis method that was first introduced in 2011 by Daubechies and Lu as an extension of the CWT and can also be applied to the STFT to improve its time-frequency resolution. [55] SST enhances the time-frequency analysis of non-stationary signals by improving the concentration of signal energy in the time-frequency domain. It addresses the inherent limitations of traditional TFRs in accurately localizing time-varying frequency components.

The SST operates by reassigning the signal energy obtained from the STFT or other TFRs to achieve improved time-frequency localization. This reassignment is achieved through a process known as synchrosqueezing, which redistributes the energy to represent the time-varying frequency components of the signal more accurately. [56]

At its core, the SST leverages the concept of instantaneous frequency, which characterizes the rate at which the frequency of a signal changes at any given time. By extracting the instantaneous frequency information, the SST enables a refined representation of the time-varying frequency content of a signal. [57]

The synchrosqueezing step involves the application of a time-frequency localization method to the STFT coefficients. This method effectively "squeezes" or concentrates the energy of the signal around its true instantaneous frequencies. One common approach for synchrosqueezing is the reassignment method, which shifts the energy content in the time-frequency plane towards the appropriate instantaneous frequency locations. [57]

The reassignment process in the SST adjusts the time and frequency coordinates of the methods' coefficients based on the estimated instantaneous frequencies. Mathematically, the reassignment operation can be expressed as follows in (16):

$$SST(t, \omega) = \sum [M(a, b)]\delta\big(t - \gamma(a, b)\big) \quad (16)$$

Where $SST(t, \omega)$ represents the synchrosqueezed transform applied to time-frequency transformation of a signal at time t and frequency ω, $M(a, b)$ denotes the time-frequency coefficient at time-frequency point (a, b), and $\gamma(a, b)$ represents the estimated instantaneous frequency associated with coefficients. The function $\delta\big(t - \gamma(a, b)\big)$ concentrates the energy of the coefficients around the estimated instantaneous frequency by shifting it to the corresponding time location. As an example, if the Synchrosqueezed Transform (SST) is applied to the STFT, the Synchro-squeezed STFT (SSQ-STFT) can be calculated using (17).

$$SSQ - STFT(t, \omega) = \sum [STFT(a, b)]\delta\big(t - \gamma(a, b)\big) \quad (17)$$

$STFT(a, b)$ denotes the STFT coefficient at time-frequency point (a, b). The instantaneous frequency, $\gamma(a, b)$ can be estimated through different approaches. one common approach is to use the phase information of the STFT coefficients.

The phase of the STFT coefficient at a particular time-frequency point (a, b) can be obtained as:

$$\phi(a, b) = \arctan\left(\frac{Im\mathrm{STFT}(a, b)}{Re\mathrm{STFT}(a, b)}\right) \quad (18)$$

Im() and Re() represent the imaginary and real parts of $STFT(a, b)$, respectively.

The estimated instantaneous frequency,$\gamma(a, b)$, can then be obtained by (19) differentiating the phase with respect to time, i.e., the derivative of the phase [52]:

$$\gamma(a,b) = \frac{d\varphi(a,b)}{dt} \tag{19}$$

The enhanced time-frequency localization provided by the SST has numerous applications in signal processing and analysis. It enables improved identification and tracking of time-varying frequency components, facilitates the detection of transient events, and enhances the separation of overlapping signal components in non-stationary signals. However, it is important to consider some of the disadvantages associated with the SST. One limitation is its computational complexity. The process of estimating instantaneous frequencies and performing energy concentration for each method's coefficient can be computationally intensive, particularly for large-scale signals or real-time applications. The SST finds applications in various fields, including audio and speech processing, biomedical signal analysis, vibration analysis, and communication systems.[58]

2.3.3.2 SET

The Synchroextracting Transform (SET) is a time-frequency analysis method that is used to study the trend and instantaneous frequency of nonlinear and nonstationary data. It is a postprocessing procedure of the STFT that can generate a more energy concentrated TFR and allow for signal reconstruction.

The SET method is inspired by the recently proposed Synchrosqueezing Transform (SST) and the theory of ideal time-frequency analysis. The main idea of SET is to only retain the time-frequency information of STFT results most related to time-varying features of the signal and to remove most smeared time-frequency energy, such that the energy concentration of the TFR can be enhanced greatly. [59]

2.3.4 Multi-Resolution Analysis

2.3.4.1 Empirical Mode Decomposition (EMD)

EMD, or Empirical Mode Decomposition, is a signal processing approach that specialises in analyzing non-stationary and nonlinear data. Huang et al. proposed it in 1998 as a data-driven strategy for dissecting signals into Intrinsic Mode Functions (IMFs). [60]

The key feature of EMD is its adaptability. It can capture signals' inherent non-stationarity by decomposing the signal into a number of IMFs that represent various oscillatory modes within the data. [61]

The EMD algorithm employs a step-by-step decomposition method. To begin, the algorithm looks for local extrema in the signal, which are points where the signal's trend changes from increasing to decreasing or vice versa. These extrema serve as a basis for the IMFs. The approach uses cubic spline interpolations to connect the local extrema, resulting in a smooth waveform that reflects the initial IMF. This is referred to as the sifting process.

After obtaining the initial IMF, it is subtracted from the original signal, leaving a residual. The algorithm then iteratively extracts successive IMFs by repeating the screening procedure on the residual. This decomposition process is repeated until the remaining signal becomes a residual, which is referred to as the final IMF. [62]

The benefits of EMD are its ability to capture signal properties at numerous scales and its adaptability to different sorts of signals. It has the potential to expose hidden oscillatory components as well as provide insights into the underlying physical processes. Furthermore, because EMD does not rely on established basis functions or assumptions about the structure of the signal, it is a versatile tool for exploratory investigation. [63]

However, EMD is not without its difficulties. One issue is mode mixing, which occurs when oscillatory components with different frequencies and scales are merged in a single IMF, making individual modes difficult to identify. Ensemble techniques, such as Ensemble EMD, have been developed to get more trustworthy decompositions in order to address this issue. Another drawback of EMD is its sensitivity to noise and lack of a solid mathematical foundation. Noise and artifacts in the signal might degrade the algorithm's performance, perhaps leading to incorrect decompositions. To offset these impacts and improve EMD accuracy, many noise-assisted approaches and noise reduction methods have been developed. [64]

Despite its limitations, EMD has a wide range of applications, including biomedical signal analysis, financial data analysis [65], and fault diagnostics in engineering systems. Because of its adaptability and capacity to find hidden patterns, it is an invaluable tool for studying and comprehending complicated and non-stationary data. [66]

2.3.4.2 Variational Mode Decomposition

Variational Mode Decomposition (VMD) is an Empirical Mode Decomposition (EMD) improvement that overcomes some of EMD's drawbacks. Dragomiretskiy and Zosso presented VMD in 2014 [67], which incorporates a regularization term to improve the mode decomposition process.

VMD extends the principles of EMD by including a regularization term to improve decomposition. In EMD, mode mixing can occur when distinct oscillatory components are combined in a single IMF during signal decomposition. VMD attempts to address this problem by reconsidering the decomposition as an optimization problem with extra constraints. [67]

The fundamental difference between VMD and EMD is in the algorithm itself. VMD handles an optimization problem utilizing a variational approach rather than iteratively sifting the signal to generate IMFs. It includes a penalty term that ensures smoothness in the decomposed modes as well as a constraint which motivates sparsity in the frequency domain. VMD intends to improve mode separation and reduce mode mixing by adding these terms. [68]

VMD has a number of advantages over EMD. For beginnings, it improves mode separation, resulting in more accurate decomposition findings. The regularization term in VMD addresses mode mixing difficulties and allows for improved isolation of specific modes, allowing for more accurate interpretation and analysis. Furthermore, VMD gives users additional control over the decomposition process by adjusting regularization settings, allowing them to customize the trade-off between smoothness and sparsity. [69]

However, VMD is not without its difficulties. The selection of proper regularization settings is one issue. Choosing the best regularization parameter values can be a subjective and iterative process that may necessitate domain expertise or extensive experimentation. Furthermore, because of the optimization problem it solves, VMD can be computationally more demanding than EMD, especially for bigger datasets. [70]

Another factor to consider is that VMD imposes more assumptions and limits than EMD. While these limits are useful in mode separation, they may not necessarily correspond to the underlying properties of the signal or capture details. As a result, it is critical to evaluate the applicability of VMD and its assumptions for the particular signal and application at hand. [71]

2.3.5 Overview of Methods

In this chapter, a complete review of the methods is offered, with numerous information in a table. The table includes information such as the year each method was introduced, an evaluation of their advantages and drawbacks in comparison to other methods, and their applicability throughout several branches.

Table 3 overview of time-frequency transformation methods

method	Year of introduction	advantages	disadvantages	application
FFT	1965	Fast computation time compared to other methods	Limited time-frequency resolution. - Not suitable for non-stationary signals	Image processing, audio processing[72]
STFT	1946	Simple and fast	Trade-off between time and frequency resolution	Speech, audio,vibration analysis[24]
CWT	1984	Better time-frequency resolution than STFT	Computationally more expensive than STFT	Seismic data feature extraction, image compression
CT	1995	analyze signals with varying frequency and amplitude modulation [73]	Computationally expensive compared to other methods such as STFT and CWT, Sensitive to noise and signal discontinuities [73]	Radar signal processing [40]
CPT	1991	better time-frequency resolution than CWT for certain types of signals [42]	Computationally more expensive than CWT [42]	Image processing, speech recognition, data

				compression [74]
WPT	1992	better time-frequency resolution than CWT for certain types of signals[75]	Computationally more expensive than CWT [75]	Detecting damage in structures like oil and gas pipelines [76], denoising [77]
WVD	1932	high time-frequency resolution compared to other methods such as STFT and CWT [78]	Cross-term interference [79]	Sound Emission feature extraction [80], electromigration noise analysis [81]
CWD	1989[53]	suppress the cross-term	Computationally expensive	Machinery diagnostics[82]
MHD	1961	Reduce interference	Computationally expensive	quantum mechanics[51], speech signal processing[83]
EMD	1998[60]	Good time-frequency resolution compared to STFT and CWT	The decomposition is not unique, sensitive to noise, produce mix-mode	Fault detection and condition monitoring[84]
VMD	2014[67]	prevent mode-mixing	The decomposition is not unique, computationally expensive.	Seismic signal processing [85]
SST	2011[55]	Good time-frequency resolution [86]compared to STFT and CWT	computationally more expensive than STFT and CWT	Seismic spectral anomaly detection[87]
SET	2019[88]	Good time-frequency resolution	Computationally expensive	Detecting epilepsy in EEG signals[89]

In summary, this chapter investigates the current level of knowledge in the sector, with a focus on the grinding process and the challenges that it presents. It also covers data collection techniques and signal transformation methods such as linear distributions, non-linear distributions, reassignment methods, and multi-resolution analysis and at the end it provided a brief overview of methods.

3. State of the research

The analysis of grinding processes has been a subject of extensive research in recent years, with significant progress made in the development of new methods for analysis. This chapter presents a thorough analysis of the application of various time-frequency transformation methods, particularly in the context of grinding processes. An overview of the state of knowledge in this area and an overview of developments in time-frequency analysis for the analysis of the grinding process are the main objectives of this chapter.

3.1 Signal transformation methods in the grinding process

In this chapter, the focus is on time-frequency transformation methods for analysing signals from grinding processes. the research on most commonly used methods is provided.

Time-frequency transformations are crucial in detecting grinding burn, which is a key concern in precision grinding procedures. These modifications enable the identification and characterization of grinding burn-related events by evaluating current, vibration, and AE signals, allowing for timely intervention and prevention of quality difficulties. [90]

3.1.1 STFT

FFT has historically been used to examine AE signals obtained during grinding experiments. [91–93] However, because it is unable to capture the time-varying frequency content, the FFT has limits when evaluating non-stationary signals like AE. [94] Alternative time-frequency analysis techniques, such the STFT, have been used to overcome this constraint. [95]

By breaking up the signals into smaller segments and performing the Fourier Transform on each segment, the STFT permits the investigation of frequency fluctuations in the AE signals over time. By showing how the frequency components change over time, this gives the signals a TFR. Researchers have created time-frequency pictures of AE signals using the STFT to get important insights about the spectrum properties of grinding burn. [96–98]

These time-frequency images, produced by the STFT analysis, show different patterns and fluctuations in frequency components, which are suggestive of the occurrence of grinding burns. Anomalies and particular frequency bands connected with grinding burn can be found by looking at how frequency content varies over time.

With the latest technologies in diagnosing and preventing heat damage during grinding processes, using the STFT in burn detection has demonstrated promising results. [96–98] Due to its computational effectiveness and strong time-frequency resolution, STFT is a frequently used technique for grinding burn detection. By examining the frequency composition of the signal, STFT can aid in the detection of grinding burns. STFT can identify changes in surface roughness and surface hardness, that are signs of grinding burn through analysing the frequency content of the signal. [90]

3.1.2 WPT

According to [99], using WPT can effectively represent AE signals that have particular properties. In particular, the multi-resolution analysis provided by WPT helps in capturing the nature of AE signals, which frequently consist of both low frequency components and short-duration high frequency bursts [100]

To show how WPTs can efficiently break down AE signals into various frequency sub-bands with varying temporal resolutions, experiments or analyses are carried out, which help in representing many properties included in the AE signals. The extraction and identification of relevant characteristics linked to high frequency bursts and low frequency components are made easier by this multi-resolution method. [101, 102]

3.1.3 EMD

The use of EMD for fault identification in grinding processes is very beneficial. It can help in the detection of grinding burn, a type of thermal damage brought on by grinding at an excessively high temperature. EMD can discover specific frequency components or patterns related to grinding burn by studying the AE signals produced during grinding. [14]

In the course of grinding, EMD can also be used to monitor and identify wheel wear. Changes in the frequency content or amplitude patterns can be used to detect wheel damage or wear by examining AE signals or vibration signals.

EMD can be used to identify chatter vibrations, which result in poor surface quality and decreased production. Chatter vibrations can be detected by unusual frequency components or amplitude modulations in the vibration or AE signals. It can be used to find imbalance in the workpiece or grinding tool. Unbalanced tool or workpiece can be detected by irregular frequency patterns or amplitude fluctuations in the vibration or AE signals. [103]

EMD can even help with spindle or grinding machine failure detection. EMD can locate frequency components or patterns connected to faults like misalignment, bearing wear, or mechanical flaws by analysing vibration signals or AE signals. [104]

In order to successfully use EMD for identifying defects in grinding processes, it is necessary to have domain knowledge, make the right sensor choices, use signal conditioning techniques, and use specific feature extraction techniques. When combined with other signal processing methods, as well as understanding of the grinding process, EMD is a useful tool.

In summary, this chapter reviews existing research on signal transformation strategies, particularly in the grinding process.

4. Evaluation of preprocessing Methods

4.1 Comparison between methods for predefined signal

The aim of this study was to evaluate different time-frequency transformation methods for processing grinding process signals and to measure their performance.

Inspiration to do this was taken from the work described in [105] to improve the evaluation of the methods that were used. The method specifically required creating an artificial signal to act as a regular reference point for evaluating the methods. It was feasible to fully understand the temporal, frequency, and amplitude characteristics of the artificial signal by making it. This information made it possible to produce a matrix that faithfully reflected the intended TFR of the signal.

It was possible to build a reference matrix against which the effectiveness of the approaches could be scientifically evaluated by using this artificial signal and its corresponding matrix representation. The matrix served as a reference instance, capturing the ideal TFR that the methods were supposed to provide. Because of this, any variations or differences between the methods' output and the expected matrix gave us important information about how well they worked.

By using this approach, it was possible to compare the methods in a uniform way and to conduct a more thorough review of the methods. A quantitative evaluation of how well the methods captured the time, frequency, and amplitude information was obtained by applying the methods to the simulated signal and contrasting their individual outputs to the desired matrix.

The reviewed methods are STFT, SSQ-STFT, CWT, Synchro-squeezed CWT (SSQ-CWT), WVD, PWVD and SET-STFT, as they were discussed before.

These approaches include a wide range of distributions, including linear, nonlinear, and reassignment methods. This deliberate decision allows for a more thorough knowledge of each type of method's working principle and its consequences for signal analysis.

The WVD was chosen as the principal method to evaluate the signal in this study because to its widespread use and proven effectiveness in studying nonstationary signals. The WVD, a nonlinear distribution approach, provides a full representation of signal time-frequency content, making it an appropriate choice for a variety of signal kinds.

Other nonlinear distribution methods, such as Zhao-Atlas-Marks, Margenau-Hill, and Choi-Williams, exist but were not used in this work. The WVD was chosen due to criteria such as its extensive use in current research, broader applicability to other signal types, and well-established theoretical foundations.

The use of the WVD, a widely established method in the area, permitted a full examination of the signal's time-frequency dynamics, contributing to current knowledge in signal processing. The use of a widely accepted approach provides a firm foundation for comparison.

It is worth noting that this research focuses on single-resolution methods rather than multi-resolution approaches such as EMD. This purposeful choice allows for a more focused analysis of the chosen methods and their specific properties, while avoiding the complication created by EMD's multi-resolution nature.

A Python code was developed specifically for this purpose to perform a comparative analysis of these time-frequency transformation methods.

To enhance computational efficiency, the ssq_stft module from the ssqueezepy package was employed, yielding simultaneous outputs of both the STFT and SSQ-STFT. The 'Hann' window function was utilized in this process, yielding favourable results. Analogously, the ssq_cwt function was leveraged to compute both the CWT and SSQ-CWT concurrently.

Additionally, the Python tftb.processing.reassigned module was used to calculate the WVD and PWVD. The pseudo_wigner_ville function, which enables the simultaneous calculation of both WVD and PWVD in a single line of code, was used to further reduce computing time. The efficiency of the analysis process for these methods was increased while the overall computing time was greatly decreased thanks to this procedure.

In order to create a non-stationary artificial signal, four overlapping sinusoidal components with constant frequencies and varying amplitudes that change across discrete time intervals were used. It is possible to determine from this signal the frequencies and related time periods at which each component displays time-varying amplitudes. The generation of signal is shown in (16).

$$x(t) = \sum_{k=1}^{N} A_k(t) \sin(2\pi f_k t) \tag{20}$$

where $A_k(t)$ represents the amplitude, which varies over time and f_k represents the frequency of the k-th component.

Each sinusoidal component has a unique frequency and amplitude, contributing to the overall 1 second signal $x(t)$. By summing these components, the resulting signal $x(t)$ exhibits a combination of different frequencies and their corresponding amplitudes.

The more precise information regarding the time intervals, frequencies, and amplitude variations can be found in the table below.

Table 4 information about artificial signal components

Component number	Time Interval (seconds)	Frequency (Hz)	Varying Amplitude
1	0.1 to 0.3	1500	Decreases linearly from 10 to 2
2	0.2 to 0.4	3000	Decreases linearly from 5 to 1
3	0.5 to 0.7	3500	Decreases linearly from 3 to 0.6
4	0.4 to 0.9	4500	Decreases linearly from 8 to 1.6

The information about how frequency and amplitude vary over time, can be extracted using TFR. Its purpose is to show how the energy of the signal is distributed in two-dimensional time-frequency space. Using this information, ideal TFR were constructed and used as a reference for evaluating the performance of each time-frequency transformation method.

The evaluation was based on parameters such as computation time, Renyi entropy and mean squared error (MSE) between the method results and the ideal TFR.

It is important to note that the assessment was carried out on a normalized matrix, guaranteeing that the results of the method and the desired matrix were both properly normalized.

As it normalized the range and distribution of values in both the desired matrix and the method's outputs, the normalization step was crucial to the evaluation. This normalizing process assisted in removing any potential inefficiencies brought on by changes in the signal's amplitude or dynamic range. A fair and equitable comparison between the desired representation and the method outputs could be made by normalizing the matrices. It was made possible by the presence of normalization in the evaluation procedure to prevent discrepancies in signal amplitudes or scales from influencing the evaluation of the methods' underlying performance and accuracy. It made it possible to compare the desired representation and method results in a more reliable and fair way, allowing for a thorough evaluation of each's performance.

computation time as am evaluation metric is used to measure the effectiveness of each method in signal processing. On the other hand, Renyi entropy was used to evaluate the accuracy and precision of the TFR generated by each method.

The diversity or richness of a signal's frequency content is quantified by renyi entropy. It is founded on the idea of information entropy, which offers a numerical assessment of how much information is there in the signal. [106]Renyi entropy can be used to describe signal complexity and is especially helpful for analysing transient behaviour of signals. The Renyi entropy of a signal can be calculated in (17):

$$H_\alpha(X) = \frac{1}{1-\alpha}\log_2 \sum_{i=1}^{n} p_i^\alpha \tag{21}$$

By using the logarithm of the probability distribution's sum raised to a power alpha, the entropy is determined.

The probability term, indicated as p_i in the context of this thesis, appears inside the logarithm in the Rényi entropy formula and symbolizes the probability of variable X in a broad sense. But in this study, the output TFR from each method replaces the place of the probability term p_i. It is necessary to normalize the replacement TFR in accordance with probability function principles.

The normalization criteria can be expressed as follows:

- The sum of all probabilities should remain unchanged:
  $\sum p_i = 1$, where i represents the index of each TFR value.
- Each probability value should fall within the range of zero to one:
  $0 \leq p_i \leq 1$, for all i.

The following equations will be used to normalize the TFR:

$$\text{scaled TFR} = \frac{\text{TFR} - \min(\text{TFR})}{\max(\text{TFR}) - \min(\text{TFR})} \tag{22}$$

In (18) the elements in the matrix are scaled to be between 0 and 1, ensuring that the first rule of a probability function is obeyed.

Furthermore, to satisfy the requirement that the sum of all elements in the matrix is equal to 1, (19) is employed:

$$\text{normalized}_{\text{TFR}} = \frac{\text{scaled TFR}}{\sum(\text{TFR})} \tag{23}$$

The entropy's sensitivity to various regions of the distribution depends on alpha's value. The Renyi entropy is best computed when alpha approaches 3 since it is more sensitive to big probabilities and less sensitive to small probabilities. This strengthens its resistance to noise and outliers. [107]

In this study, Renyi entropy was calculated for each method's output to provide a measure of how the energy is distributed in the TFR. By comparing the Renyi entropy values of each method's output, the accuracy and precision of each method could be evaluated.

Structural similarity between the method results and the desired (ideal) TFR was also calculated, providing a measure of how similar each method's output was to the reference representation. By analyzing these parameters, the performance of each method was evaluated.

The MSE is also one of the important metrics used in this thesis to evaluate how well the implemented methods performed. MSE is used as an assessment parameter in this study in order to unbiasedly assess the performance and efficacy of the implemented methods. MSE offers a thorough evaluation of the proximity between the results and the desired results by evaluating the inaccuracy between the acquired results and the desired representation and it can be calculated in (24):

$$MSE = \frac{1}{mn}\sum_{i=1}^{m}\sum_{j=1}^{n}(TFR_{des}(i,j) - TFR_{est}(i,j))^2 \tag{24}$$

Here, '*m*' represents the number of rows and '*n*' represents the number of columns of the matrices involved in the computation. TFR_{des} denotes the desired TFR matrix and TFR_{est} is the TFR that results from each method.

According to the technique described in [105], a second procedure was used in addition to MSE to assess the effectiveness of the strategies. In this process, the desired matrix was subtracted from the method output, and the ratio of zero and non-zero elements to the total number of elements in the subtracted matrix was then measured in percentage.

In this case, a subtraction value of zero in the subtracted matrix denoted that the corresponding elements in both the desired and outcome matrices were identical. This result was in complying with the intended goal, showing that the method's output and the intended representation were well aligned. As a result, a greater percentage of zeros in the subtracted matrix suggested a more precise and accurate result.

This approach added a further degree of precision and fidelity to the info obtained through MSE by taking the percentage of zeros into account. It provided insightful information on the degree of compatibility between the method results and the desired representation at the level of the individual elements. This method allowed for a more detailed evaluation, especially in situations when MSE would not adequately reflect the level of correctness.

The next stage is to add noise with different signal-to-noise ratios (SNRs) and compare the previously mentioned metrics for each method while noise is present. With this method, it is possible to evaluate how well each method can reliably capture the signal information even when there is noise present.

Each method's performance can be compared and assessed under various noise conditions by adding noise with various SNRs. This analysis aids in locating the technique that preserves robustness and accurate signal detection in the presence of noise.

Understanding how well each approach performs in real-world situations can be gained by analysing metrics such as MSE, Renyi entropy, and SSIM in the presence of noise. This makes finding a method that consistently maintains the signal's properties while reducing the effect of noise interference possible.

4.2 Comparison between methods for experimental signal

To analyse the effectiveness of time-frequency transformation algorithms in practice, it is necessary to measure their accuracy and efficiency when applied to real-world data. It is critical to ensure correct signal pre-processing before comparing the results of different algorithms on the same dataset and making relevant conclusions.

It is important to keep in mind that not all of the time-frequency transformation techniques examined in this thesis can be directly applied to the real signals utilized in the research when comparing various methods for experimental signals. This is because the signals were captured at high sampling frequencies. The vibration and current signals were captured at a frequency of 100 kHz, yielding a total of 50,000 samples for a signal duration of 0.5 seconds. The AE signals, on the other hand, were sampled at 2 MHz, producing a total of 1,000,000 samples for the identical 0.5-second period.

Memory limitations made it difficult to use several signal analysis techniques, including the WVD, on the AE signals. To handle a large number of samples, the WVD approach needs a lot of memory. However, the 1,000,000-sample AE signal was too much for the memory space that was available to handle. Down sampling reduces the signal's sample count by a certain amount. However, it was shown that the Nyquist-Shannon sampling theorem would be broken if the signal was down sampled to the degree required to solve the memory issue. The signal information would be distorted and subject to aliasing as a result of this compromise, making it unreliable for further processing. Therefore, down sampling was not an appropriate approach in this situation.

A signal cropping method was used as an alternate strategy. The AE signal had to be cropped in order to achieve the desired aim of having the same number of samples (50,000) for both the vibration, current, and AE signals. The 1,000,000 samples in the AE signals meant that only 0.025 s of the original signal could be kept for further investigation after cropping the signal to acquire 50,000 samples. The number of samples in the AE signals could be reduced to match the desired sample count by using the signal cropping approach. This made it possible to use signal analysis techniques without endangering the data's integrity. It is significant to note that only a small piece of the original signal could be kept for analysis; hence, the choice to crop the signal came with the trade-off of losing temporal information.

It should also be noted that the SET method ran into similar memory restrictions. The SET approach was unable to achieve the expected outcomes even when signal cropping was used to reduce the memory problem. This proves that memory constraints were not the only factor affecting the SET method's performance.

On the contrary to the self-generated artificial signal, where all its information was known and a desirable TFR could be established, evaluating real signals presents an individual challenge. It is essential to recognize in the context of this thesis that there is no exact detail readily available for real signals, leading to the examination of alternate ways for comparing the performance of different transformation methods. As stated in this thesis, one method of evaluating the findings is through visual comparison, in which differences between the TFRs can be visually examined and analysed.

In summary, this chapter provides a thorough examination of preprocessing approaches. It examines various approaches for both self-generated and experimental signals, evaluating their usefulness in improving data quality.

5. Discussions and results

This chapter contains the findings of the evaluation of time-frequency transformations performed to both noisy and noise-free artificial signals. The primary goal of this research was to evaluate the effectiveness of various time-frequency transformations in capturing crucial signal characteristics under varied situations.

The evaluation started with applying the time-frequency modifications to noiseless artificial signal. Each transformation method was carefully evaluated utilizing specified criteria to quantify its performance. These measures were designed expressly to assess precision, resolution, and the transformations' capacity to appropriately represent signal components across time and frequency domains.

Following that, the evaluation was expanded to include artificial signals with noise. The original signal was subjected to Gaussian noise, imitating real-world circumstances with different SNRs. This allowed us to investigate the robustness of the transformations and their capacity to attenuate the negative impacts of noise interference on the final representations. The study aims to determine the transformations' capacity to retain signal fidelity and capture significant characteristics in the face of noise by progressively raising the SNR values.

Furthermore, a restricted examination of genuine signals obtained from the grinding process was performed. While the primary focus of this research remained on artificial signal evaluation, a visual comparison was done between the TFRs generated by the transformations for both the burned case and normal case signals from the grinding process. This early investigation provided preliminary insights into the possibilities of time-frequency transformations in discriminating between different grinding operation circumstances.

5.1 Evaluation of Time-Frequency Transformations on Noise-Free Signals

5.1.1 STFT

The STFT was chosen as the tool for analysing the signal and extracting important details in this investigation. The STFT is an effective method for evaluating a signal's frequency content over time by breaking it into short, overlapping windows and applying the Fourier Transform to each window as explained in detail in chapter 2.3.1.2. This method captures both the temporal and spectral aspects of the signal.

As described in chapter 4.1, the signal under analysis is a sum of four overlapping sinusoidal components of variable amplitude. The signal was sampled at 10500 Hz.

Figures 1 and 2 show the spectrograms obtained by applying the STFT to the signal. These spectrograms depict the frequency content of the signal across time and demonstrate the inherent trade-off between time and frequency resolutions in the STFT.

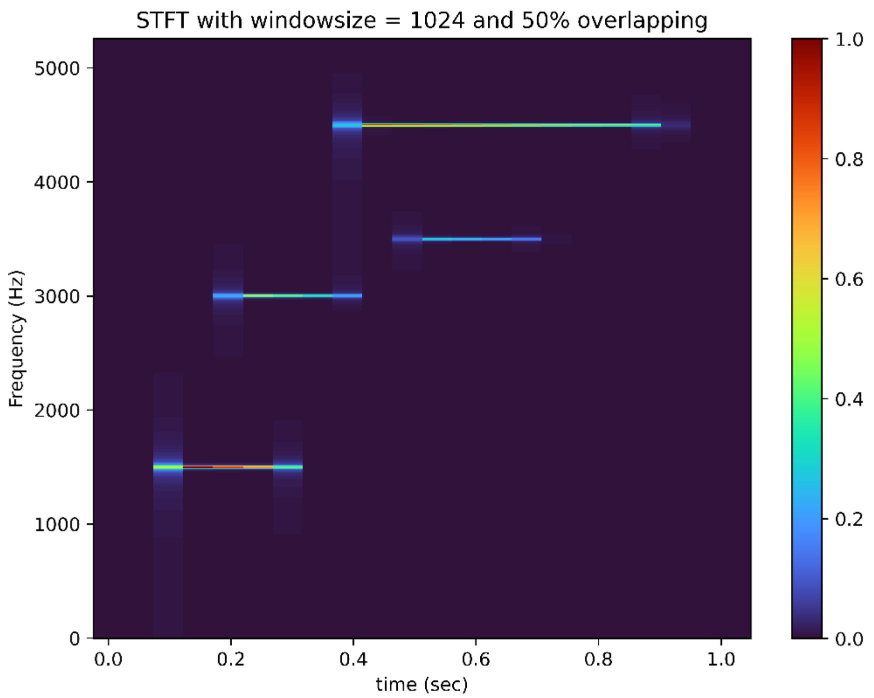

Figure 2 STFT of artificial signal with window of size= 1024 and 50% overlap

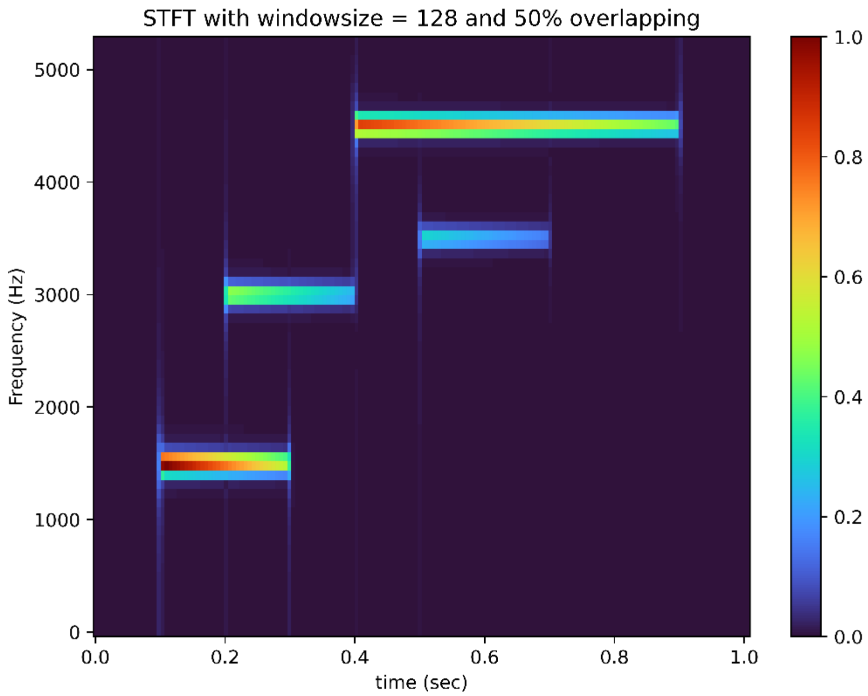

Figure 3 STFT of artificial signal with window of size = 128 and 50% overlap

The spectrogram in Figure 2 was created with a bigger window size of 1024 and 50% overlap. This configuration prioritizes frequency resolution, allowing for a more in-depth investigation of the signal's frequency content. The bigger window size improves the ability to differentiate between closely spaced frequencies but may result in slightly worse time resolution. Figure 2 displays more precise frequency information, making it ideal for looking into the finer complexities of the signal's frequency components.

Figure 3 shows the spectrogram obtained with a reduced window size of 128 and 50% overlap. This configuration prioritizes time resolution, allowing for faster changes in the signal across time. The time axis is more finely separated with the smaller window size, allowing for better viewing of temporal dynamics. The smaller window size, however, comes at the expense of poorer frequency resolution, making it more difficult to differentiate between closely spaced frequencies. From figure 3 can be concluded that the window of size 256 and 50% overlap is a good choice for capturing quick temporal shifts and overall signal trends.

Moving on to the scenario of varied overlapping sizes but the same window size, Figures 4 and 5 illustrate the spectrograms obtained with a window size of 256.

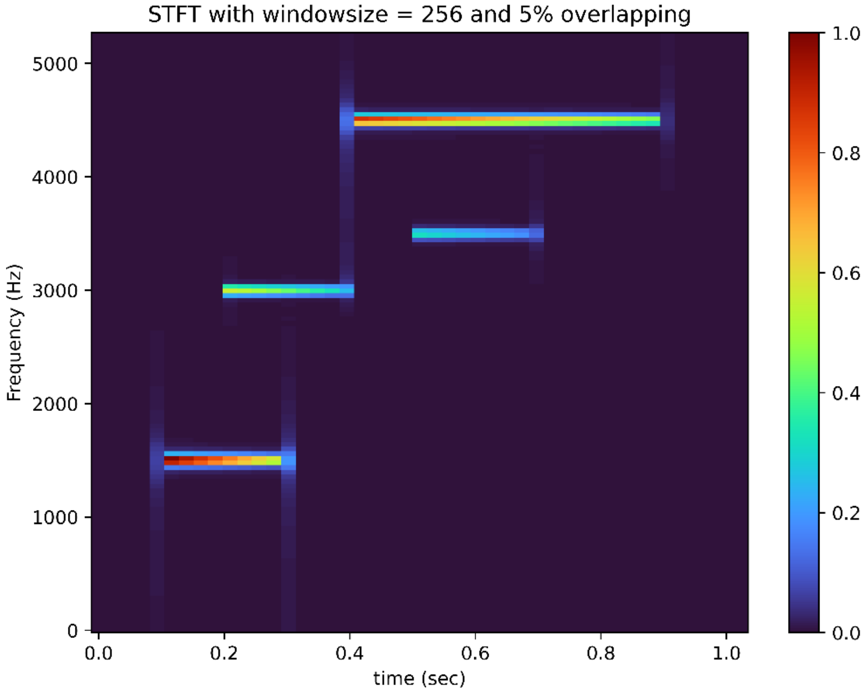

Figure 4 STFT of artificial signal with window size = 256 and 5% overlapping

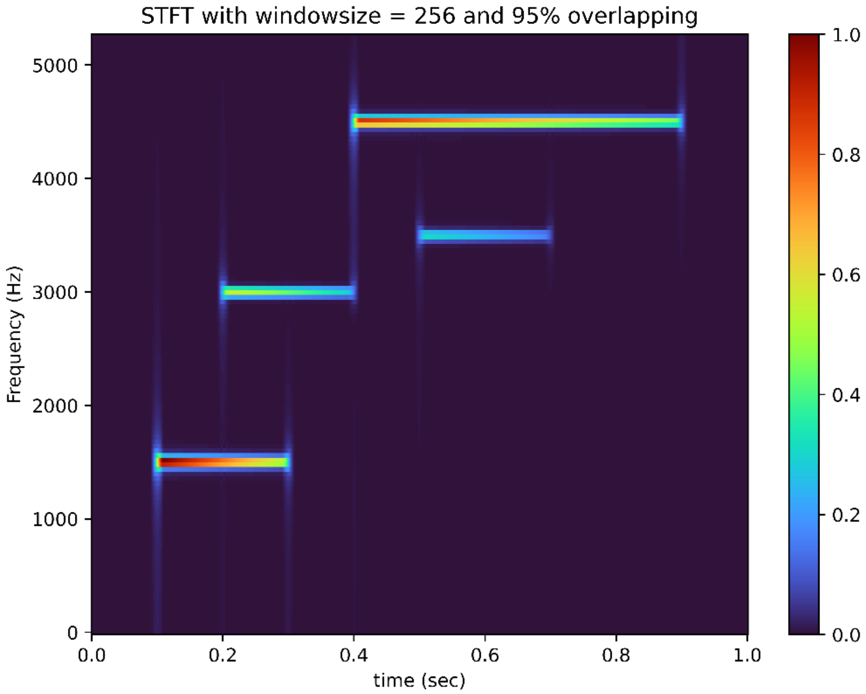

Figure 5 STFT of artificial signal with window size = 256 and 95% overlapping

Figure 4 shows a 5% overlapping spectrogram emphasizing frequency resolution. The spectrogram, with its lower overlapping size, provides a crisper depiction of the frequency content, allowing for greater distinction of closely spaced frequencies. However, by sacrificing some temporal resolution, this option is less effective at recording quick changes across time.

Figure 5 depicts the spectrogram with 95% overlap, emphasizing time resolution. The greater overlapping improves temporal dynamics visualization, allowing for the detection of rapid changes in the signal across time. This design, however, reduces frequency resolution, making it more difficult to discern between different frequencies and longer computation time.

These spectrograms demonstrate the STFT's intrinsic trade-off between time and frequency resolutions. The level of detail collected in both the temporal and frequency domains is affected by window size and overlapping. Researchers can choose the best design to extract meaningful information from the signal by carefully examining this trade-off.

5.1.2 CWT

In this chapter, the results of the CWT applied to the signal under consideration are displayed. The study focuses on the Complex Morlet wavelet, which is well-known for its advantageous qualities in a variety of applications. Sigma, which represents the standard deviation of the Gaussian envelope, is an important parameter in the Complex Morlet wavelet. The frequency and time resolution of the CWT analysis are strongly affected by the sigma value.

A detailed review of the CWT results achieved with various sigma values is provided. In particular, two situations are thoroughly examined: sigma = 6 and sigma = 20. These examples show how sigma affects the frequency and time resolution of the CWT analysis.

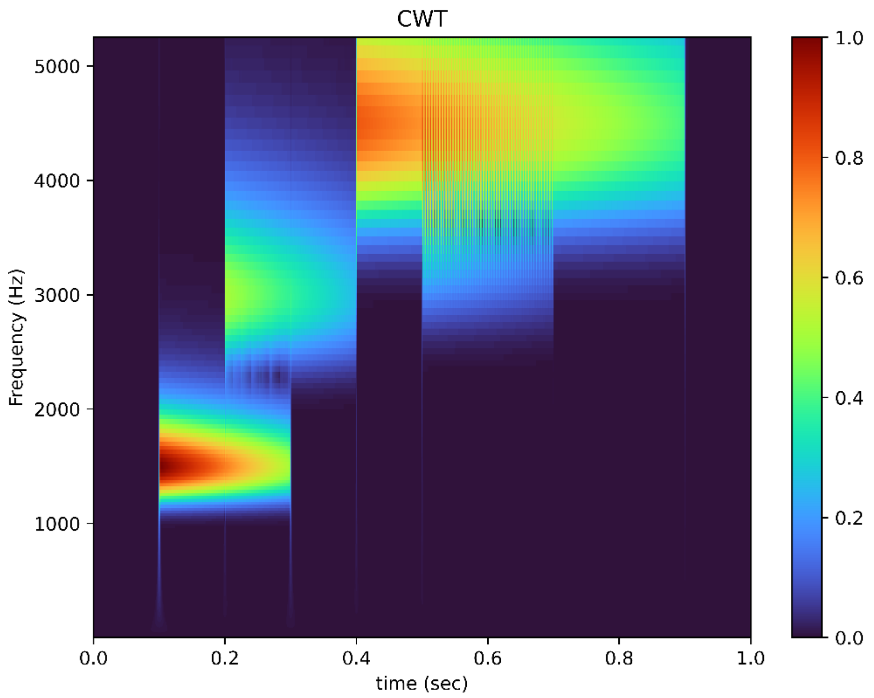

Figure 6 CWT with sigma=6

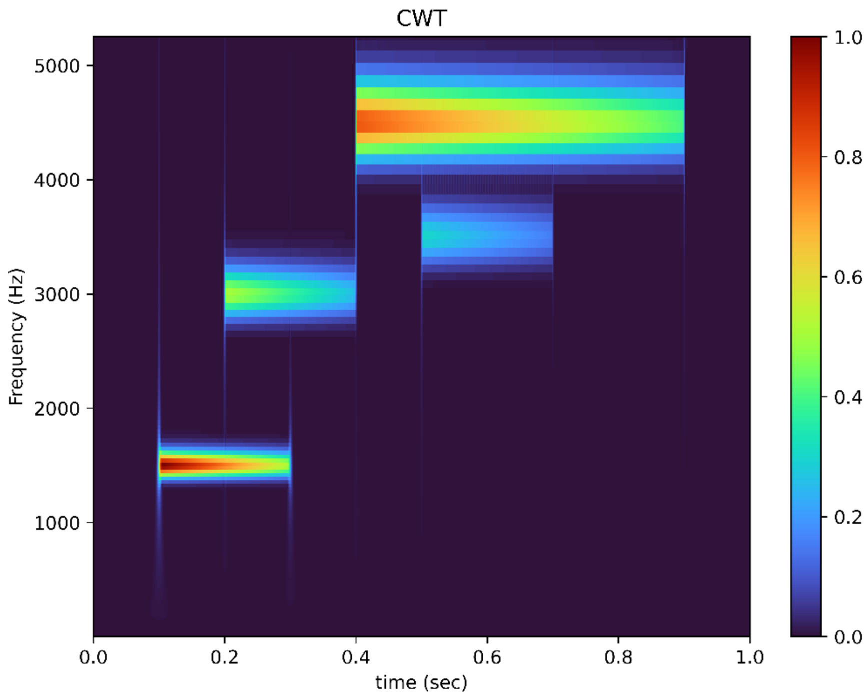

Figure 7 CWT with sigma= 20

Figure 7 shows the CWT result with sigma set to 6. The broader Gaussian envelope improves frequency resolution and allows for more exact identification of spectral features. The graphic demonstrates the CWT's capacity to disclose the signal's time-varying spectral content with more clarity.

Figure 8 shows the CWT result with sigma set to 20. This greater sigma value corresponds to a narrower Gaussian envelope, resulting in better time resolution. The frequency resolution is noticeably improved as compared to the sigma = 6 scenario. The CWT analysis detects small fluctuations in frequency components, resulting in a more complete representation of the signal's spectral content.

The influence on frequency resolution in the CWT analysis is demonstrated by increasing sigma from 6 to 20. The use of a wider Gaussian envelope allows the CWT to catch more cycles for low-frequency oscillations, allowing for improved discriminating between different frequency components. This improved frequency resolution allows for a more precise definition of the signal's spectral composition, especially for lower frequency components.

When increasing sigma, it is crucial to examine the trade-off with time resolution. Higher sigma values cause the wavelet's time localization to decrease, resulting in a broader spread of energy in the time domain. Regardless of this trade-off, the higher frequency resolution produced by using tighter Gaussian envelopes is critical for effectively collecting high-frequency components.

5.1.3 WVD and PWVD

The WVD is a time-frequency analysis approach that is often used to investigate a signal's joint time and frequency properties. It provides extensive information about how a signal's frequency components evolve over time as explained in chapter 2.3.2.1

The WVD was applied to a real-valued signal created throughout the experimental phase of this study. The TFR obtained from applying the WVD to the real signal is shown in figure 9. Notably, when applied to a real-valued signal, the resulting TFR typically becomes symmetric.

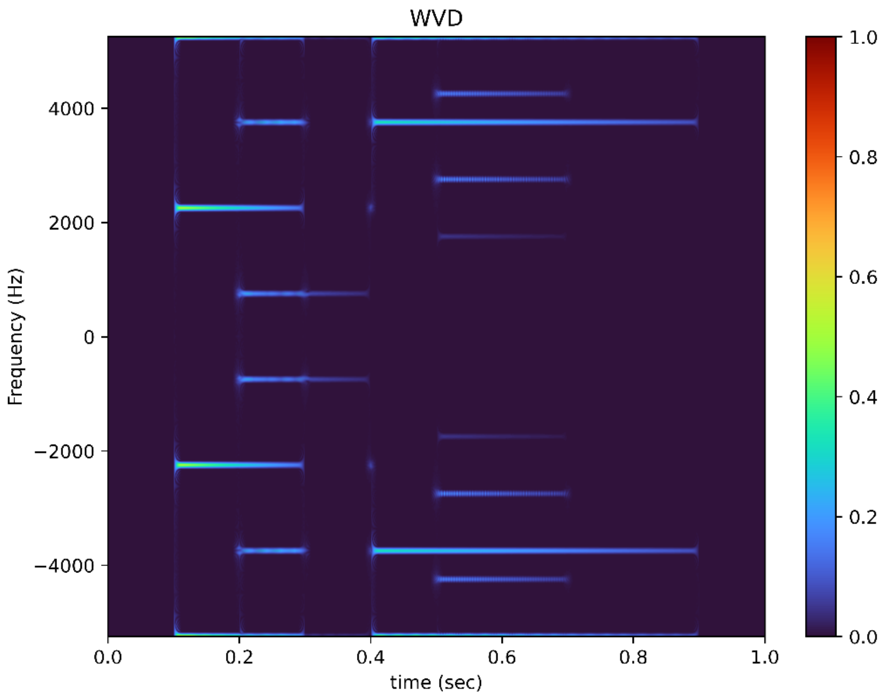

Figure 8 WVD of real signal

The observed symmetry in the TFR can be mathematically explained. For a real signal x(t), the WVD equation is in (8) defined.

When the WVD equation is expanded, $x^*(t-\tau/2)$ represents the complex conjugate of the signal $x(t-\tau/2)$, introducing symmetry into the WVD. In particular, thzero-frequencyugate of a real signal reflects the frequency components in the complex plane around the zero frequency axis.

As a result, when evaluating the WVD of a real signal, the positive and negative frequency components in the time-frequency plane symmetrically mirror each other around the zero frequency axis, resulting in the observed symmetric nature of the TFR.

To overcome the problem of comprehending the symmetric TFR, the Hilbert transform was applied to the original real signal to produce an analytical signal. The Hilbert transform removes the negative frequency components, resulting in an analytical signal with a single-sided spectrum.

Figure 10 depicts the TFR derived by applying the WVD to the analytical signal acquired by the Hilbert transform. The TFR of the analytical signal is significantly different from the TFR of the real signal. When negative frequencies are removed from the analytical signal, the TFR becomes asymmetric. This adjustment improves the TFR's interpretability by providing a clearer representation of the signal's time-varying frequency content.

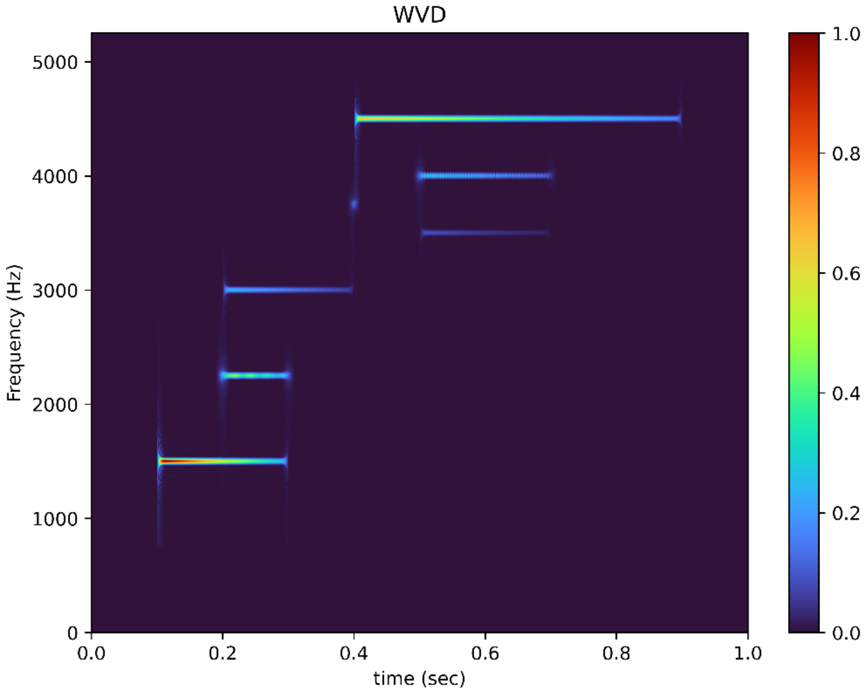

Figure 9 WVD of analytic signal

While the WVD provides strong frequency resolution and records the signal's time-frequency characteristics, it is critical to recognize the existence of interference in the overlapping regions of sinusoidal components. These interferences, which can be seen in figure 10, emerge as interference terms in the WVD output, introducing new spectral components and potentially causing TFR distortions.

One method for mitigating interference effects and improving TFR interpretability is to use the pseudo-Wigner-Ville distribution (PWVD). The PWVD is a WVD modification that includes a smoothing function to minimize interference terms as explained in chapter 2.3.2.1. The interference effects can be decreased by using a proper smoothing window in the PWVD computation, resulting in a cleaner and more concentrated representation of the signal's time-frequency content. Figure 9 depicts the outcome of applying the PWVD to the signal. When compared to Figure 8, the interference component is greatly reduced, resulting in a more accurate representation of the signal’s time-frequency properties.

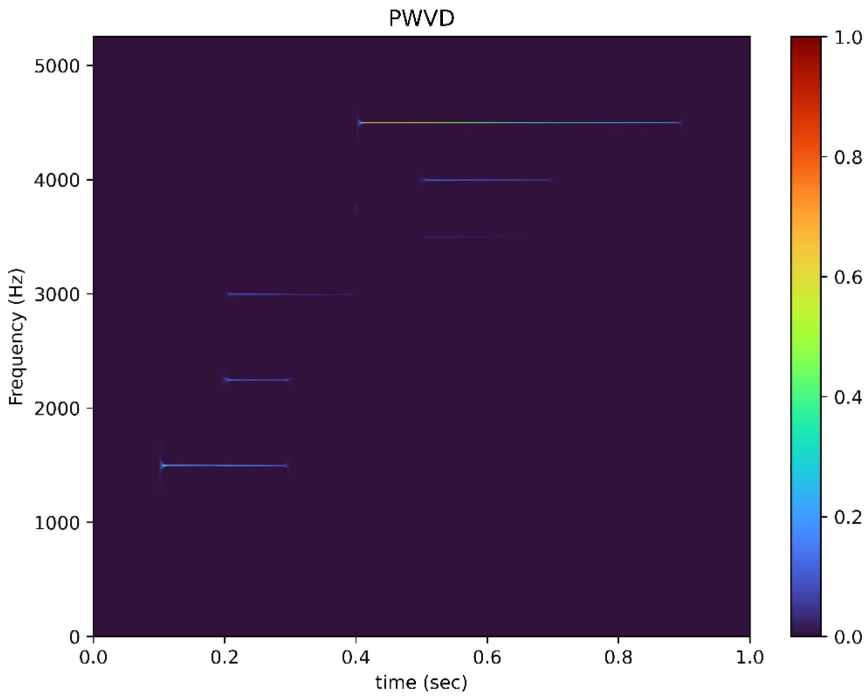

Figure 10 PWVD of analytical signal

Using the PWVD or other interference-suppressing techniques can help alleviate the interference problem identified in the WVD and offer an enhanced TFR, allowing for easier analysis and interpretation of the signal's time-frequency characteristics.

5.1.4 SSQ-STFT

The Synchro Squeezed Transform (SST) is a time-frequency analysis approach that improves the STFT in terms of frequency resolution. The results of applying the SST to the STFT are shown in this part, and they are contrasted to the standard STFT to illustrate the improved frequency resolution achieved by the SST.

Figure 12 shows the spectrogram derived from the signal's STFT, whereas Figure 13 shows the spectrogram obtained from the SST applied to the STFT. A comparison of the two spectrograms demonstrates that the SST achieves better frequency resolution.

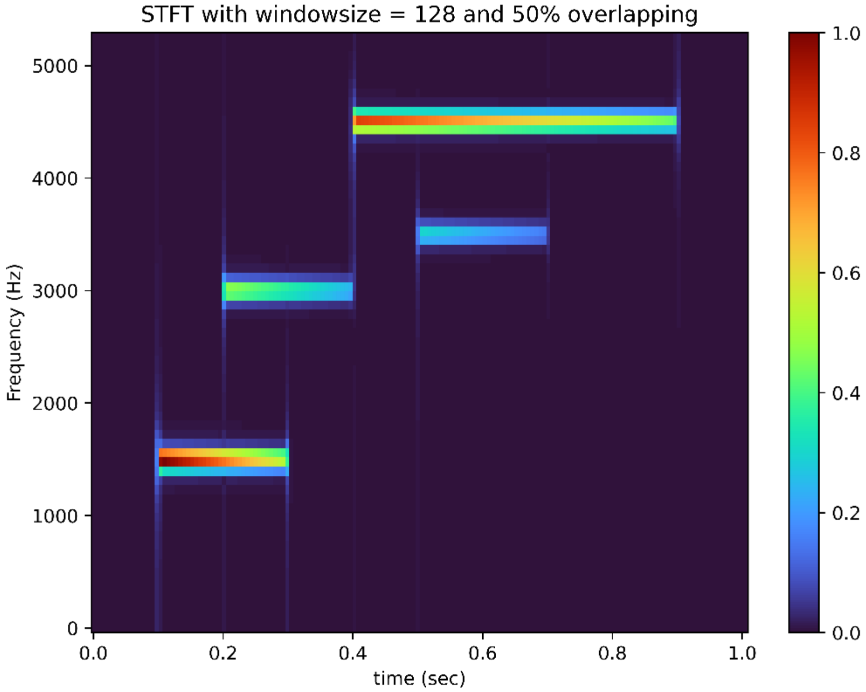

Figure 11 STFT without synchrosqueezing with window of size = 128 and 50% overlap

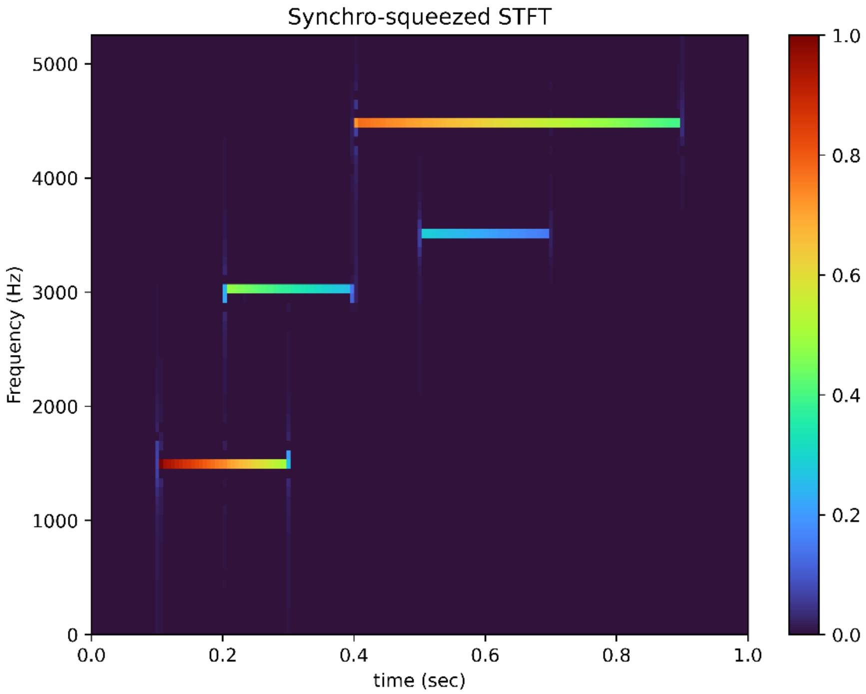

Figure 12 SSQ-STFT with window of size = 128 and 50% overlap

The STFT spectrogram in Figure 12 shows larger frequency components and less exact localization, which corresponds to the inherent trade-off between time and frequency precision. Figure 13, on the other hand, shows a narrower and more focused representation of the signal's frequency content as a result of the SST's adaptive squeezing effect. In the time-frequency plane, the frequency components appear sharper and better distinguished, offering a clearer depiction of their evolution across time.

The SST's improved frequency resolution allows for the identification of finer features and small variations in the frequency content of the signal that may not be visible in the STFT spectrogram.

It is important to note that the adaptive squeezing mechanism in the SST increases computing complexity in the STFT. However, the benefits of higher frequency resolution outweigh the extra computing cost, especially in circumstances where fine-grained time-frequency analysis is critical.

5.1.5 SSQ-CWT

This chapter provides the findings and analysis of applying the SST to the CWT using the artificial signal defined in the previous chapters of this thesis. The emphasis is on comparing the results of the SST applied to the CWT with those of the normal CWT, notably assessing the SST's greater frequency resolution.

Figure 14 illustrates the TFR obtained for the experimental dataset using the traditional CWT. The CWT captures time-varying spectral information but has limits in frequency resolution and exact localization of frequency components. The energy distribution in the time-frequency plane frequently leads to overlapping and smeared representations, making it difficult to distinguish individual frequency components and their temporal fluctuations.

In order to overcome these constraints, the SST is applied to the CWT. The SST redistributes the energy of CWT coefficients depending on local estimations of the instantaneous frequency, providing a more accurate representation of the time-varying spectral content. Figure 15 shows the resulting TFR, exhibiting the SST's improved frequency resolution and frequency component localization.

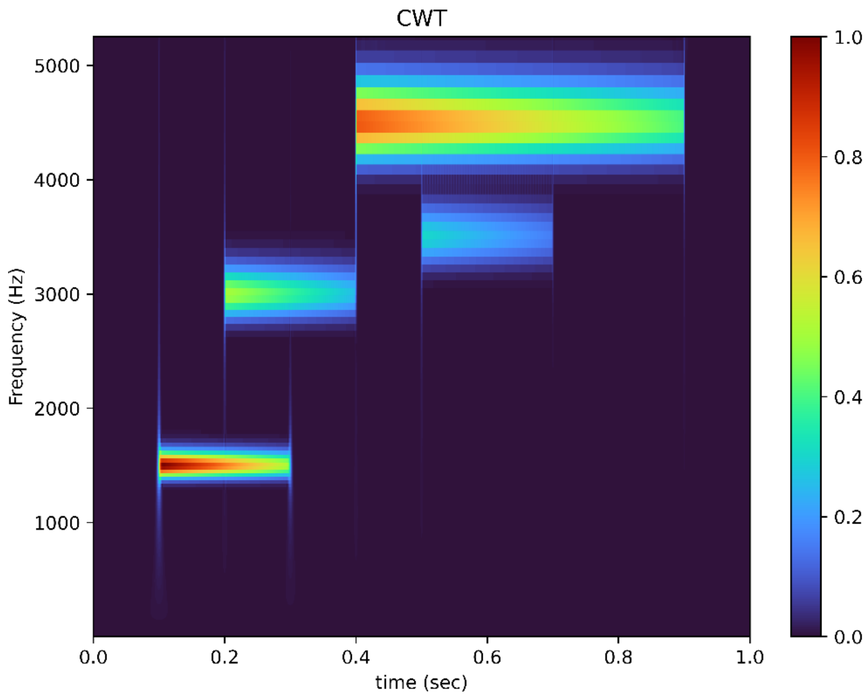

Figure 13 CWT without synchrosqueezing

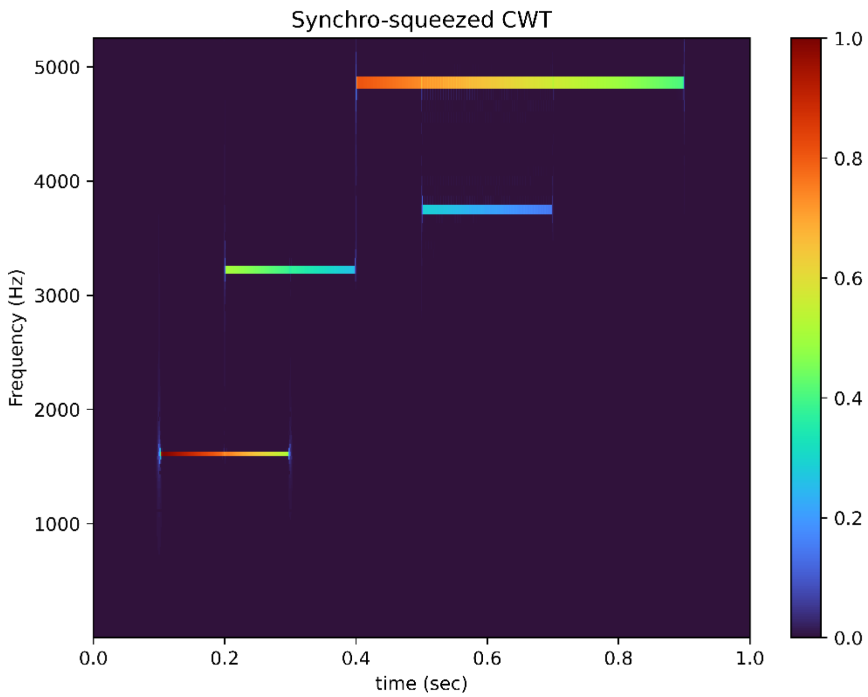

Figure 14 SSQ-CWT

The comparison of Figures 14 and 15 clearly shows the higher frequency resolution attained by the SST applied to the CWT. The improved clarity allows for a more precise examination of the time-varying spectral content, making it easier to identify essential frequency characteristics and their dynamic behaviour.

It is crucial to note that, while the SST has advantages in terms of frequency resolution and time-frequency localization, it has a higher computing complexity than the standard CWT.

5.1.6 Performance Evaluation of Time-Frequency Transformations on Noise-Free Signals

In this chapter, a variety of metrics were used to evaluate and compare the effectiveness of various time-frequency transformations. First, as described in chapter 4.1, an ideal TFR was generated. The MSE was then calculated by contrasting each method's output with the desired TFR, as described in chapter 3.1.

The desired TFR can be seen in figure 15.

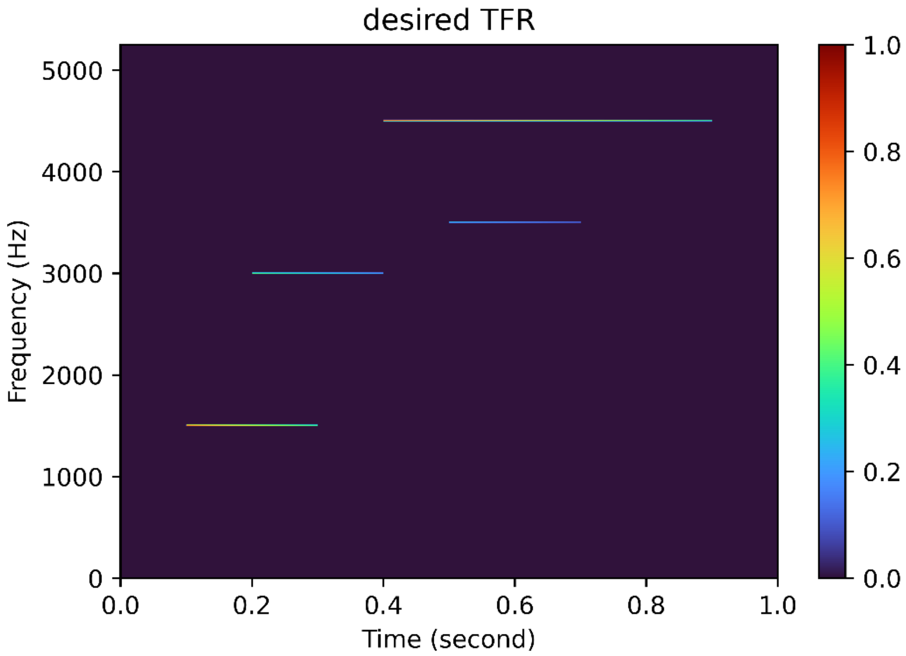

Figure 15 desired TFR

To gain more understanding of the characteristics of the TFRs generated by the various approaches, the Renyi entropy of each result was also computed and compared. Each method's computation time was tracked in order to assess its effectiveness and computational complexity. In addition, the desired TFR was subtracted from the results of each method, and the percentage of zero-elements in the subtracted matrix was analyzed. The method's output is said to be more likely to produce the desired TFR when the percentage of zero-elements is larger. This data, along with the MSE, offer a more thorough assessment of the effectiveness of the methods.

Table 5 Performance Evaluation Metrics

Method	Zero element %	Non-zero element %	MSE	Renyi Entropy	Computation time (s)
STFT	97.23	2.77	0.000423	6.3951	0.0009
SSQ-STFT	96.12	3.88	0.000917	5.1257	0.1314
WVD	96.83	3.17	0.000653	15.9487	39.2155
PWVD	97.02	2.98	0.000524	12.7582	
CWT	87.54	12.46	0.010412	15.9195	1.3250
SSQ-CWT	91.83	8.17	0.001272	12.5387	
SET	99.67	0.33	0.000006	12.3702	570.0608

The choice of an appropriate time-frequency analysis approach is highly influenced by computation time. As can be seen from the table, STFT, SSQ-STFT, PWVD, and SET all have commendably quick computation times, demonstrating their effectiveness in handling TFRs. The shortest computation time is for STFT, followed by SSQ-STFT. PWVD and SET, however, take considerably longer to compute. It is essential to note that the computation times for CWT and SSQ-CWT are provided as a single combined value as explained before in chapter 5.1, indicating that the extra steps in SSQ-CWT do not considerably increase the overall computation time when compared to CWT alone.

the entropy values of WVD, CWT, and SET are considerably greater, which denotes a more distributed dispersion of energy along the time-frequency plane. STFT, SSQ-STFT, PWVD, and SSQ-CWT, on the other hand, have lower entropy values, indicating a more concentrated or focused energy distribution. These entropy values are an accurate reflection of the unique qualities and effectiveness of each method in capturing the time-frequency information of the signal.

The MSE and percentage of zero elements provide a linked analysis of the correctness and agreement between the results of the method and the desired TFR. A closer match to the desired TFR and greater level of accuracy in capturing the time-frequency characteristics of the signal are shown by STFT, SSQ-STFT, PWVD, and SET's considerably lower MSE values. Furthermore, these techniques exhibit higher proportions of zero elements, demonstrating a higher degree of accordance.

5.2 Evaluation of Time-Frequency Transformations on Noisy Signals

This section investigates the effects of Gaussian noise on the performance of the time-frequency transformations covered in earlier sections. The signal utilized in the evaluation is distorted with Gaussian noise at various SNRs ranging from 0 to 30 dB.

The goal of this analysis is to evaluate the robustness and reliability of various time-frequency transformations by comparing outcomes achieved under noisy situations. The evaluation includes a look at the metrics outlined in Section 3.1, which provide quantitative measures of the quality and correctness of the TFRs.

Analysing the performance measures across different SNR levels can provide significant insights into how time-frequency transformations handle noise and their ability to preserve the underlying signal features. This analysis attempts to provide a better understanding of the trade-offs between noise robustness and frequency resolution, as well as to evaluate the overall performance of time-frequency transformations in practical scenarios with varied amounts of noise.

5.2.1 Quantitative Comparison of TFRs

In order to evaluate each method's effectiveness quantitatively, the MSE was computed at various SNR levels. The MSE measures how different each method's TFR is from the ideal representation as explained in section 3.1.

the relationship between MSE versus SNR variation is illustrated in Figure (16). The SNR values are shown on the x-axis, while the MSE values are shown on the y-axis. Each approach is shown as a single line, allowing for a direct evaluation of how well it performs.

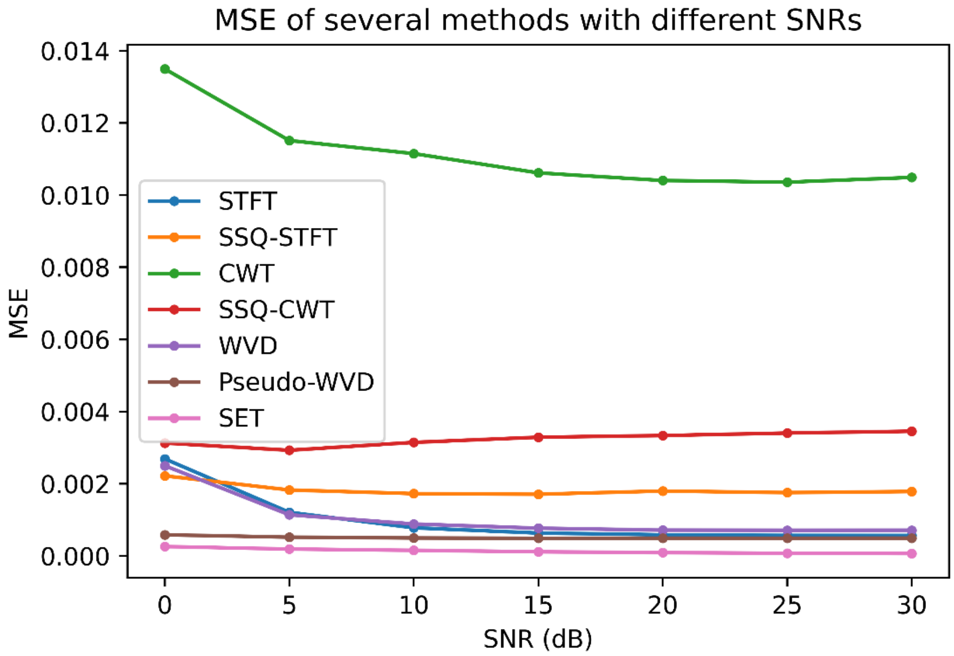

Figure 16 MSE between each method's result and ideal TFR vs. varying SNR

The evaluation's findings show that the methods' effectiveness varies. The durability of the STFT approach in precisely constructing TFR of the signal in the presence of noise is demonstrated by its consistent display of a reasonably low MSE across all SNR levels.

The MSE values for the CWT approach are somewhat greater than those for the STFT, indicating a significantly lower level of TFR construction accuracy. However, it continues to function very well, especially at greater SNR levels, demonstrating its capacity to reasonably capture the time-frequency characteristics of the signal.

The WVD approach exhibits comparable MSE values to the STFT, which is an indication of how well it reconstructs the TFR of the signal.

In comparison to the STFT and CWT approaches, the PWVD method displays substantially lower MSE values, indicating a higher level of TFR construction accuracy. Its enhanced performance is aided by its capacity to increase time-frequency resolution and suppress cross-terms.

The MSE values displayed by the SSQ-STFT and SSQ-CWT methods are comparable to those of the STFT and CWT methods, respectively. These methods use reassigned TFRs, which improves frequency component localization and boosts time-frequency concentration.

The SET approach has the lowest MSE values of all the tested methods, indicating higher reconstruction accuracy. The great performance of the SET approach is due to its ability to collect multicomponent signals with overlapping frequency components.

Analysing the Renyi entropy values for each approach at various SNR levels was the next part of the evaluation procedure. The complexity or randomness of the TFR produced by each method is quantified by the Renyi entropy. Understanding how Renyi entropy and SNR relate to one another will help for better understanding how each method characterizes and depicts the signal.

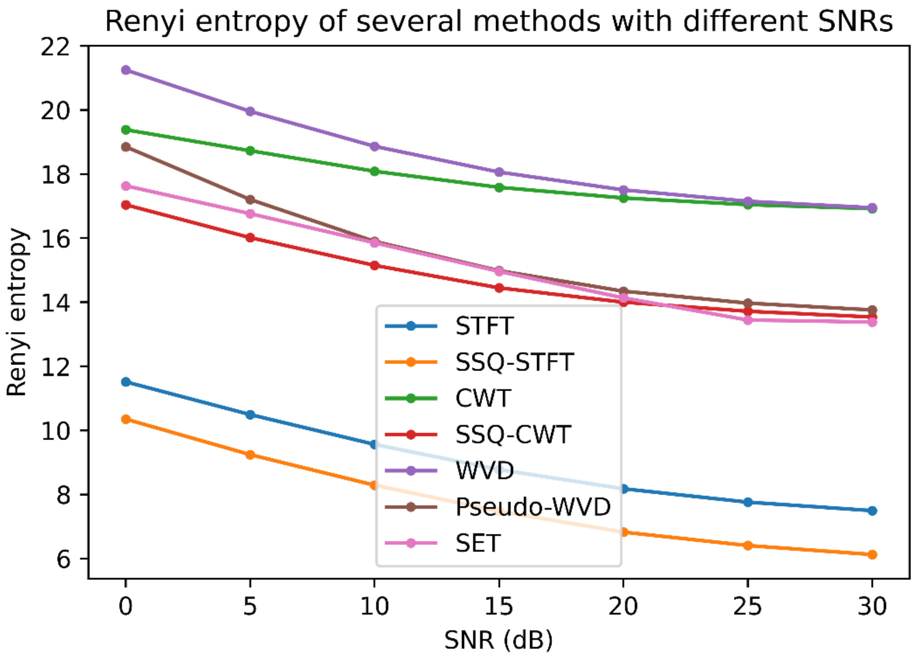

Figure 17 Renyi Entropy of resulting TFRs from each method vs. varying SNR

Figure (17) illustrates a consistent pattern of declining Renyi entropy with rising SNR across all methods. Given that noise results in amplitude scattering over the TFR, which increases randomness and raises Renyi entropy values, such a pattern is expected. On the other hand, lower Renyi entropy values are produced by lower SNR levels, which denote reduced noise and more organized signals. The theoretical knowledge of Renyi entropy and its connection to signal quality is consistent with this overall trend.

Compared to the other methods, STFT shows a considerable amount of randomness. Renyi entropy estimates for STFT show a drop in complexity or randomness with increasing SNR. In contrast, STFT typically produces larger

Renyi entropy values than certain methods, indicating that it captures some intrinsic unpredictability in the signal.

Compared to STFT, CWT exhibits a higher level of randomness. Even though CWT displays more randomness than STFT, other methods have even greater Renyi entropy values, indicating that they can capture signals with more complex properties.

Comparing STFT with CWT, WVD consistently exhibits a higher level of variability. When compared to most other approaches, WVD regularly displays greater Renyi entropy values, demonstrating its capacity to capture a variety of signal properties and variations.

When compared to STFT and WVD in terms of Renyi entropy, PWVD demonstrates a moderate to high level of randomness. Due to its capacity to reduce interferences and cross-terms that are present in the WVD, PWVD has a lower Renyi entropy than WVD, which results in a more focused representation of the signal's time-frequency components. PWVD improves the signal's clarity and distinctness by reducing undesired interference, which leads to a noticeably lower Renyi entropy.

Across various SNR levels, SSQ-STFT consistently displays the lowest Renyi entropy values. According to the Renyi entropy metric, this shows that the SSQ-STFT provides a TFR with the least amount of unpredictability or complexity. Renyi entropy results show superior performance than STFT, indicating the capacity to concentrate the signal's energy in time-frequency space.

Similar to PWVD, SSQ-CWT exhibits a moderate to high level of variability. Synchro compressed CWT generally produces slightly lower Renyi entropy values, despite similarities to PWVD, indicating a more concentrated representation of signal constituents.

SET exhibits the greatest Renyi entropy values of all of the methods that have been studied. This demonstrates its capacity to capture complicated and sophisticated signal properties. The underlying statistical characteristics and probability distributions of the amplitudes lead to the higher Renyi entropy values even though its TFR does not appear to have high entropy.

In conclusion, this chapter presents the outcomes of evaluating time-frequency transformations on noise-free and noisy signals. It examines the performance of several approaches such as MSE, Renyi Entropy and Computation time for methods, including STFT, CWT, Wigner-Ville Distribution (WVD), Pseudo Wigner-Ville Distribution (PWVD), Short-Time Synchro Squeezed Transform (SSQ-STFT), and Short-Time Synchro Compressed Wavelet Transform (SSQ-CWT).

6. Conclusion

Finally, the purpose of this study was to evaluate the performance of various time-frequency transformation approaches in detecting characteristics associated with grinding burn. The evaluation included a MSE study to measure the accuracy of TFRs, as well as a Renyi entropy examination to quantify the complexity and randomness of the created representations.

The STFT consistently demonstrated a low MSE across all SNR levels, suggesting its capacity to reliably create TFRs even in the presence of noise. Furthermore, the STFT technique exhibited reduced renyi entropy, indicating a more focussed and concentrated energy distribution in TFR. This property of the STFT approach implies that it captures the intrinsic qualities of the signal with less unpredictability.

Compared to the STFT approach, the CWT demonstrated a higher amount of randomness. Other time-frequency transformation methods, such as the WVD, PWVD, SSQ-STFT, and SSQ-CWT, demonstrated varying degrees of accuracy and unpredictability.

Among all the investigated approaches, the SET approach had the highest TFR construction accuracy with the lowest MSE values. However, due to its long computation time, SET may not be suited for this application.

While the evaluation focuses on accuracy and unpredictability, other considerations such as computing time must also be considered. The STFT approach proved not only good overall performance but also faster processing, making it a viable solution for real-time monitoring applications.

Finally, this research provides important insights into the performance of several time-frequency transformation algorithms for character recognition in grinding burn. The results indicate that the STFT approach, due to its overall good performance in terms of accuracy and calculation time, could be a viable option for this application. Nonetheless, more research is needed to investigate alternative methods that may be more suited to the processing of high-frequency signals and solve the issues observed in this work, taking factors such as accuracy, unpredictability, and computation time into account.

7. References

[1] R. K. Leach and S. T. Smith, *Basics of precision engineering*. Boca Raton, FL: CRC Press, Taylor & Francis Group, 2018.

[2] J. P. Davim, Ed., *Microfabrication and precision engineering: Research and development*. Amsterdam: Elsevier, 2017.

[3] T. Mohanraj, S. Shankar, R. Rajasekar, N. R. Sakthivel, and A. Pramanik, "Tool condition monitoring techniques in milling process — a review," *Journal of Materials Research and Technology*, vol. 9, no. 1, pp. 1032–1042, 2020, doi: 10.1016/j.jmrt.2019.10.031.

[4] K. Xu *et al.*, "Advanced Data Collection and Analysis in Data-Driven Manufacturing Process," (in En;en), *Chin. J. Mech. Eng.*, vol. 33, no. 1, pp. 1–21, 2020, doi: 10.1186/s10033-020-00459-x.

[5] C. H. Lauro, L. C. Brandão, D. Baldo, R. A. Reis, and J. P. Davim, "Monitoring and processing signal applied in machining processes – A review," *Measurement*, vol. 58, pp. 73–86, 2014, doi: 10.1016/j.measurement.2014.08.035.

[6] D. Goyal, C. Mongia, and S. Sehgal, "Applications of Digital Signal Processing in Monitoring Machining Processes and Rotary Components: A Review," *IEEE Sensors J.*, vol. 21, no. 7, pp. 8780–8804, 2021, doi: 10.1109/JSEN.2021.3050718.

[7] J. Yuan, L. Liu, Z. Yang, J. Bo, and Y. Zhang, "Tool wear condition monitoring by combining spindle motor current signal analysis and machined surface image processing," *Int J Adv Manuf Technol*, vol. 116, 7-8, pp. 2697–2709, 2021, doi: 10.1007/s00170-021-07366-y.

[8] S. A. Abdelwahab, "Surface Roughness Modeling and Prediction Based on Vibration Signal Analysis and Machining Parameters in Milling of Aluminum by Artificial Neural Network," *J. Inst. Eng. India Ser. C*, vol. 104, no. 2, pp. 345–375, 2023, doi: 10.1007/s40032-023-00924-1.

[9] M. Kuntoğlu, E. Salur, M. K. Gupta, M. Sarıkaya, and D. Y. Pimenov, "A state-of-the-art review on sensors and signal processing systems in mechanical machining processes," *Int J Adv Manuf Technol*, vol. 116, 9-10, pp. 2711–2735, 2021, doi: 10.1007/s00170-021-07425-4.

[10] L. O'Toole, C.-W. Kang, and F.-Z. Fang, "Precision micro-milling process: state of the art," *Adv. Manuf.*, vol. 9, no. 2, pp. 173–205, 2021, doi: 10.1007/s40436-020-00323-0.

[11] E. O. Ezugwu, "Key improvements in the machining of difficult-to-cut aerospace superalloys," *International Journal of Machine Tools and Manufacture*, vol. 45, 12-13, pp. 1353–1367, 2005, doi: 10.1016/j.ijmachtools.2005.02.003.

[12] S. Malkin, "Grinding Processes," in *Encyclopedia of tribology: With 3650 figures and 493 tablets*, Q. Wang and Y.-W. Chung, Eds., New York: SpringerReference, 2013, pp. 1573–1580.

[13] B. Denkena, T. Ortmaier, M. Ahrens, and R. Fischer, "Monitoring of grinding wheel defects using recursive estimation," (in En;en), *Int J Adv Manuf Technol*, vol. 75, 5-8, pp. 1005–1015, 2014, doi: 10.1007/s00170-014-6170-3.

[14] E. Sauter, E. Sarikaya, M. Winter, and K. Wegener, "In-process detection of grinding burn using machine learning," (in En;en), *Int J Adv Manuf Technol*, vol. 115, 7-8, pp. 2281–2297, 2021, doi: 10.1007/s00170-021-06896-9.

[15] "Monitoring of grinding burn by AE and vibration signals," *ICAART 2014 - Proceedings of the 6th International Conference on Agents and Artificial Intelligence*,

pp. 272–279, 2014. [Online]. Available: https://repositorio.unesp.br/handle/11449/171598

[16] R. Kuppuswamy, F. Jani, S. Naidoo, and Q. de Jongh, “A study on intelligent grinding systems with industrial perspective,” (in En;en), *Int J Adv Manuf Technol*, vol. 115, 11-12, pp. 3811–3827, 2021, doi: 10.1007/s00170-021-07315-9.

[17] R. Thomazella, W. N. Lopes, P. R. Aguiar, F. A. Alexandre, A. A. Fiocchi, and E. C. Bianchi, *Digital signal processing for self-vibration monitoring in grinding: A new approach based on the time-frequency analysis of vibration signals*, 2019. [Online]. Available: https://www.researchgate.net/publication/333439384_Digital_signal_processing_for_self-vibration_monitoring_in_grinding_A_new_approach_based_on_the_time-frequency_analysis_of_vibration_signals

[18] H. K. Tönshoff, T. Friemuth, and J. C. Becker, “Process Monitoring in Grinding,” *CIRP Annals*, vol. 51, no. 2, pp. 551–571, 2002, doi: 10.1016/S0007-8506(07)61700-4.

[19] Y. Hong, S. Xiu, C. Sun, Y. Zhao, and X. Zhang, “Metallographic method for temperature measurement: Reconstruction of grinding temperature field based on critical austenitizing depth and cyclic feedback algorithm,” *Journal of Materials Processing Technology*, vol. 310, p. 117770, 2022, doi: 10.1016/j.jmatprotec.2022.117770.

[20] X. Kong, S. Xiu, C. Sun, Y. Yao, X. Zou, and Y. Zhao, “Study on the relevance of strengthened layer and vibration signal in grinding-strengthening process,” *Int J Adv Manuf Technol*, vol. 121, 11-12, pp. 7963–7982, 2022, doi: 10.1007/s00170-022-09730-y.

[21] L. Stanković, M. Daković, and T. Thayaparan, *Time-frequency signal analysis with applications*. Boston, [Piscataqay, New Jersey]: Artech House; IEEE Xplore, 2013. [Online]. Available: http://ieeexplore.ieee.org/document/9100932

[22] A. F. Harvey and M. Cerna, “The Fundamentals of FFT-Based Signal Analysis and Measurement in LabVIEW and LabWindows,” 1993. [Online]. Available: https://www.semanticscholar.org/paper/The-Fundamentals-of-FFT-Based-Signal-Analysis-and-Harvey-Cerna/9aaac129f06ae0079d803fb30829e2f594d95a3f

[23] K. Pal, *Bioelectronics and medical devices: From materials to devices - fabrication, applications and reliability / edited by Kunal Pal [and six others]*. Oxford: Woodhead Publishing, 2019.

[24] D. Gabor, “Theory of communication. Part 1: The analysis of information,” *Journal of the Institution of Electrical Engineers - Part III: Radio and Communication Engineering*, vol. 93, no. 26, pp. 429–441, 1946, doi: 10.1049/ji-3-2.1946.0074.

[25] A. Akan and O. Karabiber Cura, “Time–frequency signal processing: Today and future,” *Digital Signal Processing*, vol. 119, p. 103216, 2021, doi: 10.1016/j.dsp.2021.103216.

[26] P. K. Ghosh and T. V. Sreenivas, “Time-varying filter interpretation of Fourier transform and its variants,” *Signal Processing*, vol. 86, no. 11, pp. 3258–3263, 2006, doi: 10.1016/j.sigpro.2006.01.005.

[27] M. Varanis, A. L. Silva, J. M. Balthazar, and R. Pederiva, “A Tutorial Review on Time-Frequency Analysis of Non-Stationary Vibration Signals with Nonlinear Dynamics Applications,” (in En;en), *Braz J Phys*, vol. 51, no. 3, pp. 859–877, 2021, doi: 10.1007/s13538-020-00842-y.

[28] C. Mateo and J. A. Talavera, “Short-time Fourier transform with the window size fixed in the frequency domain,” *Digital Signal Processing*, vol. 77, pp. 13–21, 2018, doi: 10.1016/j.dsp.2017.11.003.

[29] K. R. Borisagar, R. M. Thanki, and B. S. Sedani, “Fourier Transform, Short-Time Fourier Transform, and Wavelet Transform,” in *Speech enhancement techniques for digital hearing aids*, K. R. Borisagar, R. M. Thanki, and B. S. Sedani, Eds., Cham: Springer, 2019, pp. 63–74.

[30] E. Rubio and J. C. Jáuregui-Correa, “A Wavelet Approach to Estimate The Quality of Ground Parts,” *JART*, vol. 10, no. 1, 2012, doi: 10.22201/icat.16656423.2012.10.1.418.

[31] N. Bajaj, “Wavelets for EEG Analysis,” in *Wavelet theory*, S. Mohammady, Ed., London: IntechOpen, 2021.

[32] L. Debnath and F. A. Shah, *Wavelet transforms and their applications*. New York: Birkhäuser, 2014.

[33] M. X. Cohen, “A better way to define and describe Morlet wavelets for time-frequency analysis,” *NeuroImage*, vol. 199, pp. 81–86, 2019, doi: 10.1016/j.neuroimage.2019.05.048.

[34] F. K. Chan, A. W. Fu, and C. Yu, “Haar wavelets for efficient similarity search of time-series: with and without time warping,” *IEEE Trans. Knowl. Data Eng.*, vol. 15, no. 3, pp. 686–705, 2003, doi: 10.1109/TKDE.2003.1198399.

[35] H. Li, “Complex Morlet wavelet amplitude and phase map based bearing fault diagnosis,” in *Eighth World Congress on Intelligent Control and Automation, WCICA 2010, 7-9 July 2010*, Jinan, China, 2010, pp. 6923–6926.

[36] M. Rhif, A. Ben Abbes, I. Farah, B. Martínez, and Y. Sang, “Wavelet Transform Application for/in Non-Stationary Time-Series Analysis: A Review,” *Applied Sciences*, vol. 9, no. 7, p. 1345, 2019, doi: 10.3390/app9071345.

[37] J. Ashmead, “Morlet Wavelets in Quantum Mechanics,” *Quanta*, vol. 1, no. 1, 2012, doi: 10.12743/quanta.v1i1.5.

[38] S. Mann and S. Haykin, “Time-frequency perspectives: the 'chirplet' transform,” in *ICASSP-92: 17th International conference on acoustics, speech and signal processing : Papers*, San Francisco, CA, USA, 1992, 417-420 vol.3.

[39] F. Millioz and M. Davies, “Sparse Detection in the Chirplet Transform: Application to FMCW Radar Signals,” *IEEE Transactions on Signal Processing*, vol. 60, no. 6, pp. 2800–2813, 2012, doi: 10.1109/TSP.2012.2190730.

[40] X. Zhu, B. Li, K. Yang, Z. Zhang, and W. Li, “High-resolution chirplet transform: from parameters analysis to parameters combination,” Aug. 2021. [Online]. Available: https://arxiv.org/pdf/2108.00572

[41] C. Zhang, Y. Chen, and W. Tan, “Discrete Cosine Wavelet Packet Transform and Its Application in Compressed Sensing for Speech Signal,” in *2012 Fourth International Symposium on Information Science and Engineering*, 2012, pp. 144–148.

[42] P. Prakasam and M. Madheswaran, “Adaptive algorithm for speech Compression using Cosine Packet Transform,” in *ICIAS 2007: International Conference on Intelligent and Advanced Systems KL Convention Center, Kuala Lumpur, Malaysia, 25-28 November 2007*, Kuala Lumpur, 2007, pp. 1168–1172.

[43] R. X. Gao and R. Yan, *Wavelets: Theory and applications for manufacturing / by Robert X. Gao, Ruqiang Yan*. New York, London: Springer, 2010.

[44] S. A. A. Karim, M. H. Kamarudin, B. A. Karim, M. K. Hasan, and J. Sulaiman, “Wavelet Transform and Fast Fourier Transform for signal compression: A comparative study,” in *2011 International Conference on Electronic Devices, Systems and Applications (ICESDA 2011): Kuala Lumpur, Malaysia, 25-27 April 2011 ; [proceedings]*, Kuala Lumpur, Malaysia, 2011, pp. 280–285.

[45] L. Cohen, “Time-frequency distributions-a review,” *Proc. IEEE*, vol. 77, no. 7, pp. 941–981, 1989, doi: 10.1109/5.30749.

[46] H. Li, H. Zheng, and L. Tang, “Wigner-Ville Distribution Based on EMD for Faults Diagnosis of Bearing,” in 2006, pp. 803–812. [Online]. Available: https://link.springer.com/chapter/10.1007/11881599_99

[47] B. Zhang and S. Sato, “A time-frequency distribution of Cohen's class with a compound kernel and its application to speech signal processing,” *IEEE Trans. Signal Process.*, vol. 42, no. 1, pp. 54–64, 1994, doi: 10.1109/78.258121.

[48] L. Debnath, “The Wigner-Ville Distribution and Time-Frequency Signal Analysis,” in *Wavelet Transforms and Their Applications*: Birkhäuser, Boston, MA, 2002, pp. 307–360. [Online]. Available: https://link.springer.com/chapter/10.1007/978-1-4612-0097-0_5
[49] X. Hua and J. Liu, “A novel fast algorithm for the pseudo Winger–Ville distribution,” (in En;en), *J. Commun. Technol. Electron.*, vol. 60, no. 11, pp. 1238–1247, 2015, doi: 10.1134/S1064226915110054.
[50] Y. Liu, P. Wu, A. W. Black, and G. K. Anumanchipalli, “A Fast and Accurate Pitch Estimation Algorithm Based on the Pseudo Wigner-Ville Distribution,” Oct. 2022. [Online]. Available: https://arxiv.org/pdf/2210.15272
[51] H. Margenau and R. N. Hill, “Correlation between Measurements in Quantum Theory,” *Prog. Theor. Phys.*, vol. 26, no. 5, pp. 722–738, 1961, doi: 10.1143/PTP.26.722.
[52] E. Sejdić, I. Djurović, and J. Jiang, “Time–frequency feature representation using energy concentration: An overview of recent advances,” *Digital Signal Processing*, vol. 19, no. 1, pp. 153–183, 2009, doi: 10.1016/j.dsp.2007.12.004.
[53] H.-I. Choi and W. J. Williams, “Improved time-frequency representation of multicomponent signals using exponential kernels,” *IEEE Transactions on Acoustics, Speech, and Signal Processing*, vol. 37, no. 6, pp. 862–871, 1989, doi: 10.1109/ASSP.1989.28057.
[54] D. T. Barry, “Fast calculation of the Choi-Williams time-frequency distribution,” *IEEE Trans. Signal Process.*, vol. 40, no. 2, pp. 450–455, 1992, doi: 10.1109/78.124957.
[55] I. Daubechies, J. Lu, and H.-T. Wu, “Synchrosqueezed wavelet transforms: An empirical mode decomposition-like tool,” *Applied and Computational Harmonic Analysis*, vol. 30, no. 2, pp. 243–261, 2011, doi: 10.1016/j.acha.2010.08.002.
[56] Y. Lv, B. Pan, C. Yi, and Y. Ma, “A Novel Fault Feature Recognition Method for Time-Varying Signals and Its Application to Planetary Gearbox Fault Diagnosis under Variable Speed Conditions,” *Sensors (Basel, Switzerland)*, vol. 19, no. 14, 2019, doi: 10.3390/s19143154.
[57] Q. Jiang, A. Prater-Bennette, B. W. Suter, and A. Zeyani, “Instantaneous Frequency-Embedded Synchrosqueezing Transform for Signal Separation,” *Front. Appl. Math. Stat.*, vol. 8, 2022, doi: 10.3389/fams.2022.830530.
[58] S. Meignen, T. Oberlin, and D.-H. Pham, “Synchrosqueezing transforms: From low- to high-frequency modulations and perspectives,” *Comptes Rendus Physique*, vol. 20, no. 5, pp. 449–460, 2019, doi: 10.1016/j.crhy.2019.07.001.
[59] G. Yu, M. Yu, and C. Xu, “Synchroextracting Transform,” *IEEE Transactions on Industrial Electronics*, vol. 64, no. 10, pp. 8042–8054, 2017, doi: 10.1109/TIE.2017.2696503.
[60] N. E. Huang *et al.*, “The empirical mode decomposition and the Hilbert spectrum for nonlinear and non-stationary time series analysis,” *Proc. R. Soc. Lond. A*, vol. 454, no. 1971, pp. 903–995, 1998, doi: 10.1098/rspa.1998.0193.
[61] L. Lin and J. Hongbing, “Signal feature extraction based on an improved EMD method,” *Measurement*, vol. 42, no. 5, pp. 796–803, 2009, doi: 10.1016/j.measurement.2009.01.001.
[62] T. Oberlin, S. Meignen, and V. Perrier, “An Alternative Formulation for the Empirical Mode Decomposition,” *IEEE Transactions on Signal Processing*, vol. 60, no. 5, pp. 2236–2246, 2012, doi: 10.1109/TSP.2012.2187202.
[63] E. Pinheiro, O. Postolache, and P. Girão, “Empirical Mode Decomposition and Principal Component Analysis implementation in processing non-invasive cardiovascular signals,” *Measurement*, vol. 45, no. 2, pp. 175–181, 2012, doi: 10.1016/j.measurement.2011.03.022.

[64] O. B. Fosso and M. Molinas, “EMD Mode Mixing Separation of Signals with Close Spectral Proximity in Smart Grids,” in *2018 IEEE PES Innovative Smart Grid Technologies Conference Europe (ISGT-Europe 2018): Sarajevo, Bosnia and Herzegovina, 21-25 October 2018,* Sarajevo, Bosnia and Herzegovina, 2018, pp. 1–6.
[65] Z. Jin, Y. Jin, and Z. Chen, “Empirical mode decomposition using deep learning model for financial market forecasting,” *PeerJ Computer Science*, vol. 8, e1076, 2022, doi: 10.7717/peerj-cs.1076.
[66] D. Yu, J. Cheng, and Y. Yang, “Application of EMD method and Hilbert spectrum to the fault diagnosis of roller bearings,” *Mechanical Systems and Signal Processing*, vol. 19, no. 2, pp. 259–270, 2005, doi: 10.1016/S0888-3270(03)00099-2.
[67] K. Dragomiretskiy and D. Zosso, “Variational Mode Decomposition,” *IEEE Transactions on Signal Processing*, vol. 62, no. 3, pp. 531–544, 2014, doi: 10.1109/TSP.2013.2288675.
[68] S. Yu and J. Ma, “Complex Variational Mode Decomposition for Slop-Preserving Denoising,” *IEEE Trans. Geosci. Remote Sensing*, vol. 56, no. 1, pp. 586–597, 2018, doi: 10.1109/TGRS.2017.2751642.
[69] S. Mohanty, K. K. Gupta, and K. S. Raju, “Comparative study between VMD and EMD in bearing fault diagnosis,” in *ICIIS 2014: 9th International Conference on Industrial and Information Systems : 15-17 December, 2014*, Gwalior, India, 2014, pp. 1–6.
[70] H. Li, B. Xu, F. Zhou, B. Yan, and F. Zhou, “Empirical Variational Mode Decomposition Based on Binary Tree Algorithm,” *Sensors (Basel, Switzerland)*, vol. 22, no. 13, 2022, doi: 10.3390/s22134961.
[71] M. Gan, H. Pan, Y. Chen, and S. Pan, “Application of the Variational Mode Decomposition (VMD) method to river tides,” *Estuarine, Coastal and Shelf Science*, vol. 261, p. 107570, 2021, doi: 10.1016/j.ecss.2021.107570.
[72] J. W. Cooley and J. W. Tukey, “An algorithm for the machine calculation of complex Fourier series,” *Math. Comp.*, vol. 19, no. 90, pp. 297–301, 1965, doi: 10.1090/s0025-5718-1965-0178586-1.
[73] G. Yu and Y. Zhou, “General linear chirplet transform,” *Mechanical Systems and Signal Processing*, 70-71, pp. 958–973, 2016, doi: 10.1016/j.ymssp.2015.09.004.
[74] C. Zhang, Y. Chen, and W. Tan, “Discrete Cosine Wavelet Packet Transform and Its Application in Compressed Sensing for Speech Signal,” in *2012 Fourth International Symposium on Information Science and Engineering*, 2012.
[75] D. Bianchi, E. Mayrhofer, M. Gröschl, G. Betz, and A. Vernes, “Wavelet packet transform for detection of single events in acoustic emission signals,” *Mechanical Systems and Signal Processing*, 64-65, pp. 441–451, 2015, doi: 10.1016/j.ymssp.2015.04.014.
[76] X.-L. Peng, H. Hao, and Z.-X. Li, “Application of wavelet packet transform in subsea pipeline bedding condition assessment,” *Engineering Structures*, vol. 39, pp. 50–65, 2012, doi: 10.1016/j.engstruct.2012.01.017.
[77] R. X. Gao and R. Yan, “Wavelet Packet Transform,” in *Wavelets*: Springer, Boston, MA, 2011, pp. 69–81. [Online]. Available: https://link.springer.com/chapter/10.1007/978-1-4419-1545-0_5
[78] M. Ralston, M. Rauch-Davies, K. Li-Chun, X. Hui-Ping, and Y. Di-Sheng, “General method to reduce crossterm interference in the Wigner-Ville decomposition,” in *SEG Technical Program Expanded Abstracts 2007*, 012007, pp. 870–874.
[79] Y. Wang, Y. Rao, and D. Xu, “Multichannel maximum-entropy method for the Wigner-Ville distribution,” *GEOPHYSICS*, vol. 85, no. 1, V25-V31, 2020, doi: 10.1190/geo2019-0347.1.

[80] J.-D. Wu and P.-H. Chiang, "Application of Wigner–Ville distribution and probability neural network for scooter engine fault diagnosis," *Expert Systems with Applications*, vol. 36, no. 2, pp. 2187–2199, 2009, doi: 10.1016/j.eswa.2007.12.012.
[81] C. M. Tan and S. Y. Lim, "Application of Wigner-Ville distribution in electromigration noise analysis," *IEEE Transactions on Device and Materials Reliability*, vol. 2, no. 2, pp. 30–35, 2002, doi: 10.1109/TDMR.2002.802114.
[82] H. A. Gaberson, "Application of Choi—Williams Reduced Interference Time Frequency Distribution to Machinery Diagnostics," *Shock and Vibration*, vol. 2, no. 6, pp. 437–444, 1995, doi: 10.1155/1995/721969.
[83] S. Vasudevrao, H. S. Karthik, I. Reena, Sudha, and A. R. Usha Devi, "Margenau–Hill operator valued measures and joint measurability," *Int. J. Quantum Inform.*, vol. 20, no. 07, 2022, doi: 10.1142/S021974992250023X.
[84] Y. Lei, J. Lin, Z. He, and M. J. Zuo, "A review on empirical mode decomposition in fault diagnosis of rotating machinery," *Mechanical Systems and Signal Processing*, vol. 35, 1-2, pp. 108–126, 2013, doi: 10.1016/j.ymssp.2012.09.015.
[85] W. Liu, Y. Liu, S. Li, and Y. Chen, "A Review of Variational Mode Decomposition in Seismic Data Analysis," (in En;en), *Surv Geophys*, vol. 44, no. 2, pp. 323–355, 2023, doi: 10.1007/s10712-022-09742-z.
[86] Wei Liu, Siyuan Cao, Yang Liu, and Yangkang Chen, "Synchrosqueezing transform and its applications in seismic data analysis," *Journal of Seismic Exploration*, vol. 25, no. 3, pp. 27–44, 2016. [Online]. Available: https://www.researchgate.net/publication/294874005_Synchrosqueezing_transform_and_its_applications_in_seismic_data_analysis
[87] Z. Huang, J. Zhang, T. Zhao, and Y. Sun, "Synchrosqueezing S-Transform and Its Application in Seismic Spectral Decomposition," *IEEE Trans. Geosci. Remote Sensing*, vol. 54, no. 2, pp. 817–825, 2016, doi: 10.1109/TGRS.2015.2466660.
[88] G. Yu, M. Yu, and C. Xu, "Synchroextracting Transform," *IEEE Transactions on Industrial Electronics*, vol. 64, no. 10, pp. 8042–8054, 2017, doi: 10.1109/TIE.2017.2696503.
[89] V. Rajinikanth, S. Kadry, D. Taniar, K. Kamalanand, M. A. Elaziz, and K. P. Thanaraj, "Detecting epilepsy in EEG signals using synchro-extracting-transform (SET) supported classification technique," (in En;en), *J Ambient Intell Human Comput*, pp. 1–19, 2022, doi: 10.1007/s12652-021-03676-x.
[90] H. B. Hübner, M. A. V. Duarte, and R. B. Da Silva, "Automatic grinding burn recognition based on time-frequency analysis and convolutional neural networks," (in En;en), *Int J Adv Manuf Technol*, vol. 110, 7-8, pp. 1833–1849, 2020, doi: 10.1007/s00170-020-05902-w.
[91] J.-S. Kwak and M.-K. Ha, "Neural network approach for diagnosis of grinding operation by acoustic emission and power signals," *Journal of Materials Processing Technology*, vol. 147, no. 1, pp. 65–71, 2004, doi: 10.1016/j.jmatprotec.2003.11.016.
[92] J. Kwak and Jihun Song, "Trouble diagnosis of the grinding process by using acoustic emission signals," *International Journal of Machine Tools & Manufacture*, 2001. [Online]. Available: https://www.semanticscholar.org/paper/Trouble-diagnosis-of-the-grinding-process-by-using-Kwak-Song/cbe39133f9745dca9c79460f233383c3729e98b3
[93] D. M. S. Ribeiro, P. R. Aguiar, L. F. G. Fabiano, D. M. D'Addona, F. G. Baptista, and E. C. Bianchi, "Spectra Measurements Using Piezoelectric Diaphragms to Detect Burn in Grinding Process," *IEEE Trans. Instrum. Meas.*, vol. 66, no. 11, pp. 3052–3063, 2017, doi: 10.1109/TIM.2017.2731038.
[94] Z. Yang and Z. Yu, "Grinding wheel wear monitoring based on wavelet analysis and support vector machine," (in En;en), *Int J Adv Manuf Technol*, vol. 62, 1-4, pp. 107–121, 2012, doi: 10.1007/s00170-011-3797-1.

[95] J. M. Griffin and X. Chen, “Multiple classification of the acoustic emission signals extracted during burn and chatter anomalies using genetic programming,” (in En;en), *Int J Adv Manuf Technol*, vol. 45, 11-12, pp. 1152–1168, 2009, doi: 10.1007/s00170-009-2026-7.

[96] M.-Q. Tran, M.-K. Liu, and Q.-V. Tran, “Milling chatter detection using scalogram and deep convolutional neural network,” *Int J Adv Manuf Technol*, vol. 107, 3-4, pp. 1505–1516, 2020, doi: 10.1007/s00170-019-04807-7.

[97] A. Kothuru, S. P. Nooka, and R. Liu, “Application of deep visualization in CNN-based tool condition monitoring for end milling,” *Procedia Manufacturing*, vol. 34, pp. 995–1004, 2019, doi: 10.1016/j.promfg.2019.06.096.

[98] C. Cheng, J. Li, Y. Liu, M. Nie, and W. Wang, “Deep convolutional neural network-based in-process tool condition monitoring in abrasive belt grinding,” *Computers in Industry*, vol. 106, pp. 1–13, 2019, doi: 10.1016/j.compind.2018.12.002.

[99] Q. Liu, X. Chen, and N. Gindy, “Investigation of acoustic emission signals under a simulative environment of grinding burn,” *International Journal of Machine Tools and Manufacture*, vol. 46, 3-4, pp. 284–292, 2006, doi: 10.1016/j.ijmachtools.2005.05.017.

[100] X. Li and J. Wu, “Wavelet analysis of acoustic emission signals in boring,” *Proceedings of the Institution of Mechanical Engineers, Part B: Journal of Engineering Manufacture*, vol. 214, no. 5, pp. 421–424, 2000, doi: 10.1243/0954405001518206.

[101] W. J. Staszewski and K. M. Holford, “Wavelet Signal Processing of Acoustic Emission Data,” *KEM*, 204-205, pp. 351–358, 2001, doi: 10.4028/www.scientific.net/KEM.204-205.351.

[102] Q. Liu, X. Chen, and N. Gindy, “Investigation of acoustic emission signals under a simulative environment of grinding burn,” *International Journal of Machine Tools and Manufacture*, vol. 46, 3-4, pp. 284–292, 2006, doi: 10.1016/j.ijmachtools.2005.05.017.

[103] W. Guo, B. Li, S. Shen, and Q. Zhou, “An intelligent grinding burn detection system based on two-stage feature selection and stacked sparse autoencoder,” (in En;en), *Int J Adv Manuf Technol*, vol. 103, 5-8, pp. 2837–2847, 2019, doi: 10.1007/s00170-019-03748-5.

[104] H.-G. Chen, J.-Y. Shen, W.-H. Chen, C.-S. Huang, Y.-Y. Yi, and J.-C. Qian, “Grinding Chatter Detection and Identification Based on BEMD and LSSVM,” (in En;en), *Chin. J. Mech. Eng.*, vol. 32, no. 1, pp. 1–13, 2019, doi: 10.1186/s10033-018-0313-7.

[105] Mariia Fedotenkova and Axel Hutt, “Research report: Comparison of different time-frequency representations,” 2014.

[106] X. Mao, P. Shang, J. Wang, and Y. Ma, “Characterizing time series by extended complexity-entropy curves based on Tsallis, Rényi, and power spectral entropy,” *Chaos (Woodbury, N.Y.)*, vol. 28, no. 11, p. 113106, 2018, doi: 10.1063/1.5038758.

[107] J. Lerga, N. Saulig, and V. Mozetič, “Algorithm based on the short-term Rényi entropy and IF estimation for noisy EEG signals analysis,” *Computers in biology and medicine*, vol. 80, pp. 1–13, 2017, doi: 10.1016/j.compbiomed.2016.11.002.

List of tables

List of figures

List of symbols and abbreviations

AE ....*Acoustic Emission*
CT.. *Chirplet Transform*
CWT... *Continuous Wavelet Transform*
EMD...Empirical Mode Decomposition
FFT..*Fast Fourier Transform*
MSE ....*Mean Squared Error*
PWVD... *Pseudo Wigner-Ville Distribution*
SNR.. *Signal to Noise Ratio*
SSQ-CWT .... *Synchro-squeezed CWT*
SSQ-STFT...*Synchro-squeezed STFT*
SST.. *Synchro-Squeezed Transform*
STFT .... *Short Time Fourier Transform*
TFR ....*Time-Frequency Representation*
WVD .... *Wigner-Ville Distribution*